**ISSN 1526-5757**

# 18. SPHENE, MYRMEKITE, AND TITANIUM IMMOBILITY AND MOBILITY; IMPLICATIONS FOR LARGE-SCALE K- AND Na-METASOMATISM AND THE ORIGIN OF MAGNETITE CONCENTRATIONS

**Lorence G. Collins**

**email: ORUHQFHFROOLQV#PDLOFRP**

**May 19, 1997**

## Introduction

Titanium, among the other major elements (Ca, Al, Fe, Mg, Mn, K, and Na) in plutonic igneous rocks may be the *most immobile* during metasomatic processes. Field and thin section studies of the titaniferous La Quinta biotite-hornblende quartz diorite in California and the titanium-bearing Lyon Mountain clinopyroxene granite gneiss in New York confirm the relative immobility of Ti where secondary sphene has been crystallized in deformed portions of these rocks. Nevertheless, where these rocks have been strongly modified, textural relationships between sphene and other minerals suggest important implications for large-scale K- and Na-metasomatism and mobility of Ti. The mobility of Ti may also be tied in with the mobility of Fe during the formation of magnetite concentrations in New York.

## La Quinta quartz diorite, San Jacinto Mountains, California

The La Quinta biotite-hornblende quartz diorite in the San Jacinto Mountains of southern California (Fig. 2) is readily accessible along the Pines-to-Palms highway (route 74).

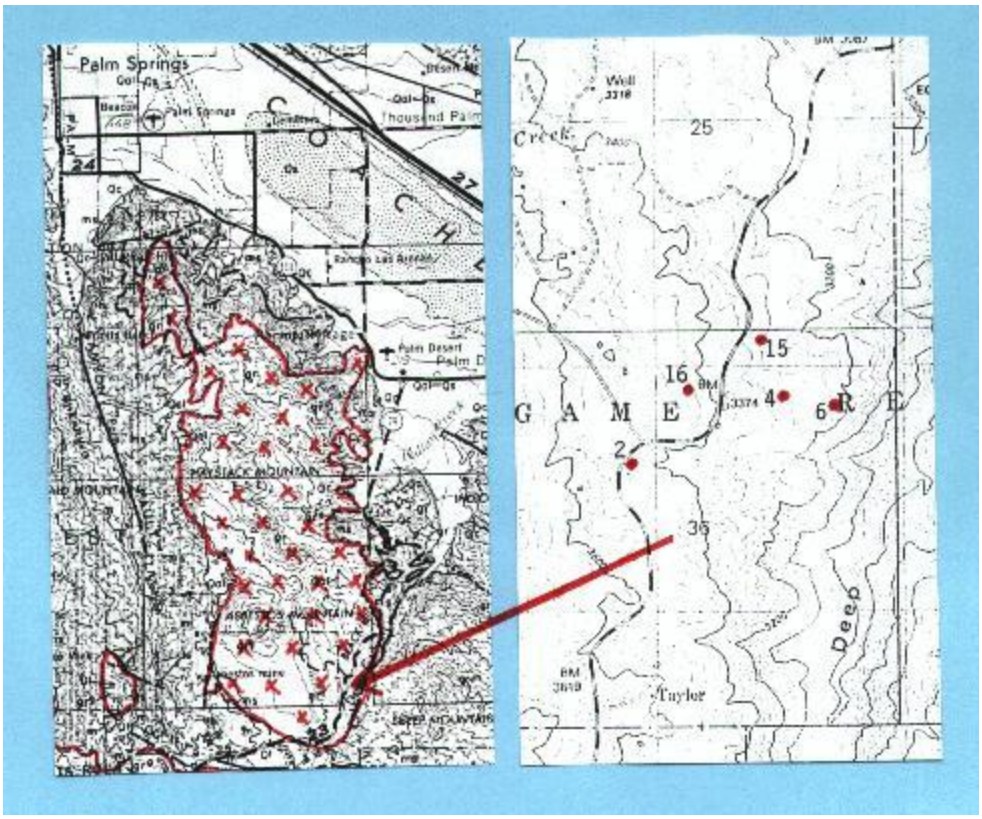


**Fig. 1.** Area southeast of Palm Springs, California, outlined in red and containing x-symbols is the La Quinta quartz diorite (map modified after a portion of the Santa Ana Sheet of the Geologic Map of California, California Division of Mines and Geology, compiled by T. H. Rogers, 1965). Location of loose sphene crystals in sandy desert soils on weathered sphene-bearing quartz diorite occurs in the east half of Section 36, T6S, R5E, of Toro Peak 7 1/2 Minute Quadrangle, California. Numbers indicate locations of chemically analyzed rocks (Table 1). Road is route 74. Contour interval is 20 feet.

This quartz diorite is gradational to granodiorite and is locally cut by granite pegmatite and aplite dikes (Geyer, 1962). Deep weathering and disintegration of these rocks produces a sandy desert soil which commonly contains loose, large, euhedral sphene crystals (Fig. 2), up to 2.5 cm long (Webb, 1939). Where these sphene crystals are present, adjacent outcrops show that the quartz diorite is deformed (gneissose), and thin sections reveal a slight to strong cataclastic texture (e.g., bent and broken albite-twin lamellae), depending on location. Where granitic aplite and pegmatite dikes (0.5 m wide) extend through the quartz diorite near the top of the valley wall of Deep Canyon (Fig. 1), as much as 10 vol. % sphene occurs in aggregates of sphene, quartz, and plagioclase crystals in the dikes. The sphene commonly contains rounded or embayed plagioclase inclusions (Fig. 3 and

Fig. 4) and is generally associated with microcline and wartlike myrmekite (Fig. 5 and Fig. 6). Primary allanite crystals in the quartz diorite are overgrown by secondary epidote (Fig. 7). In some places, an occasional hornblende crystal exhibits quartz sieve textures (Fig. 8).

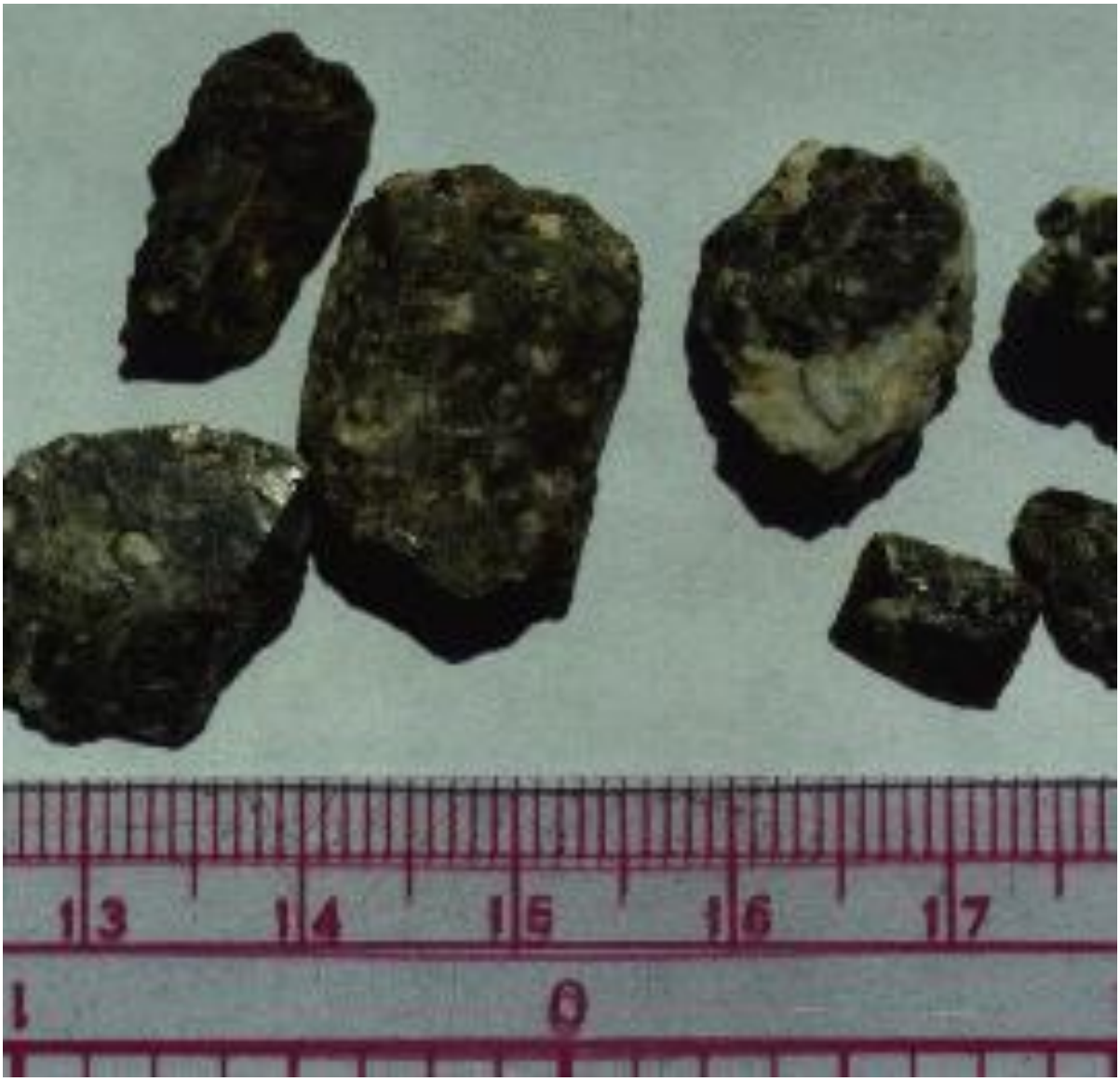


**Fig. 2.** Euhedral sphene crystals (brown), some of which are intergrown with quartz and plagioclase (white). Scale shows centimeters and inches.

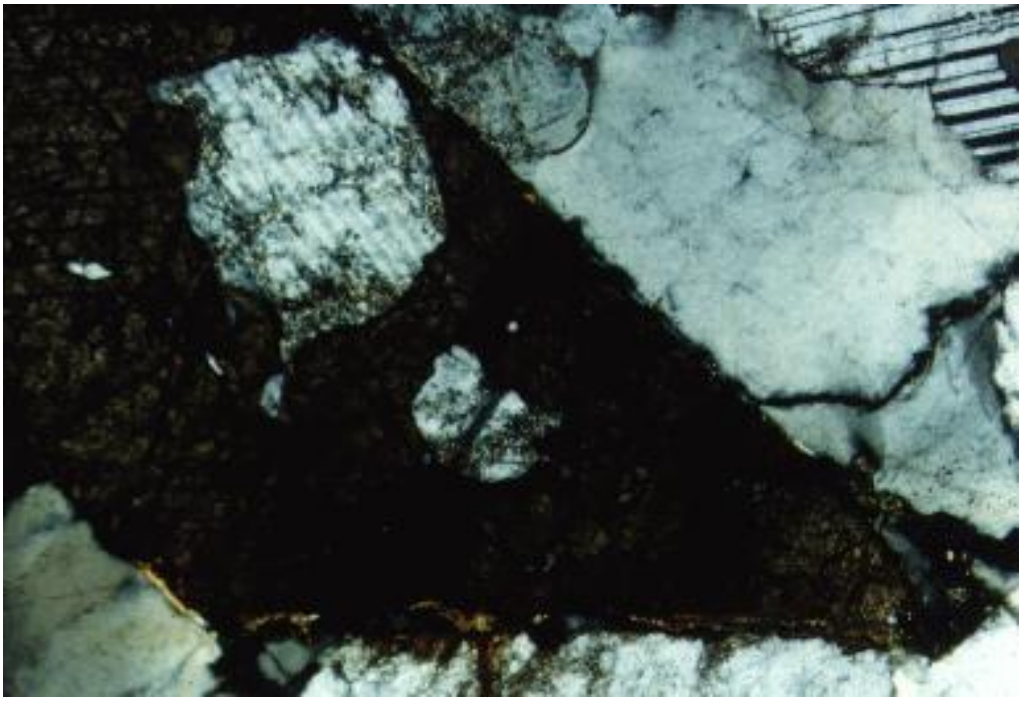

**Fig. 3.** Euhedral sphene (brown, pointed tip toward lower right) with remnant, rounded, albite-twinned plagioclase inclusions (white). Quartz (clear, rounded crystals; gray-white).

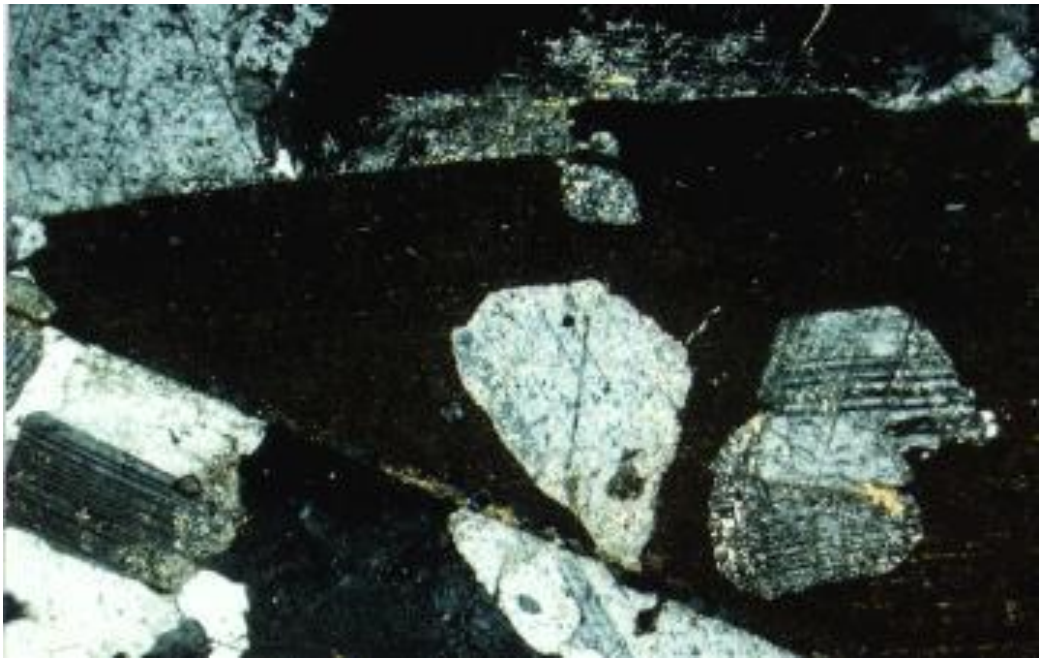

**Fig. 4.** Euhedral sphene (brown; pointed tip toward left side) with remnant, rounded, albite-twinned plagioclase inclusions (gray and white). Bordering crystals are plagioclase.

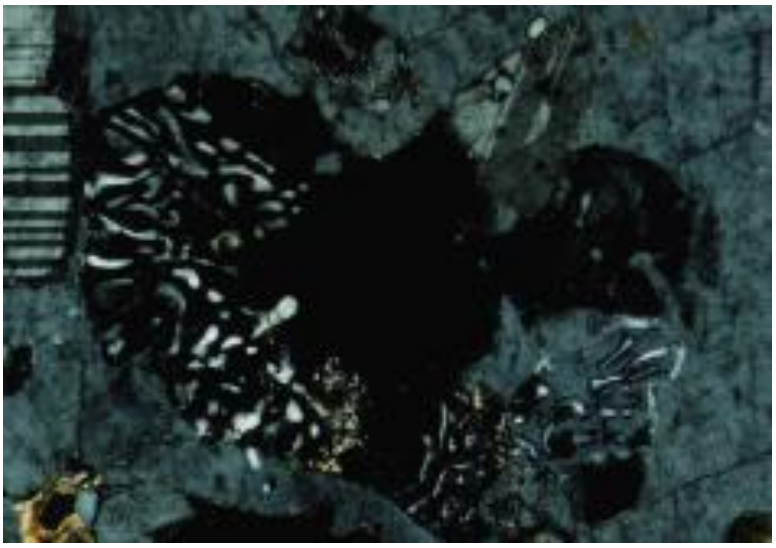

**Fig. 5.** Wartlike myrmekite projecting into microcline (gray); albite-twinned plagioclase (white and gray). Remnant quartz vermicules (white) extend into microcline adjacent to myrmekite.

**Fig. 6.** Wartlike myrmekite on borders of microcline (gray); quartz (white).

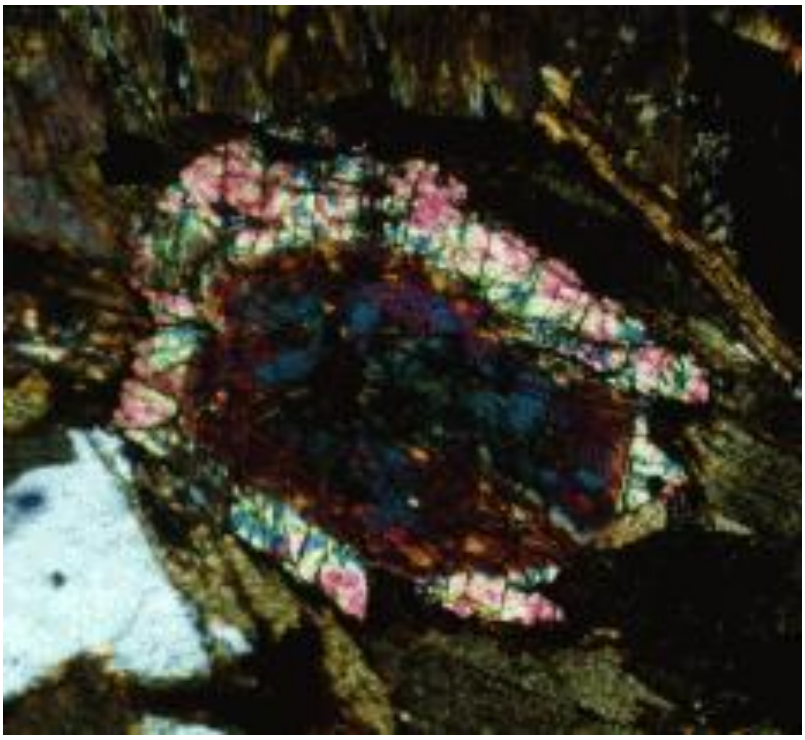

**Fig. 7.** Allanite (center; blue, maroon, brown) with an overgrowth of epidote (pink, yellow, green), surrounded by biotite (brown, tan; lower right) and hornblende (brown; upper left); quartz (white).

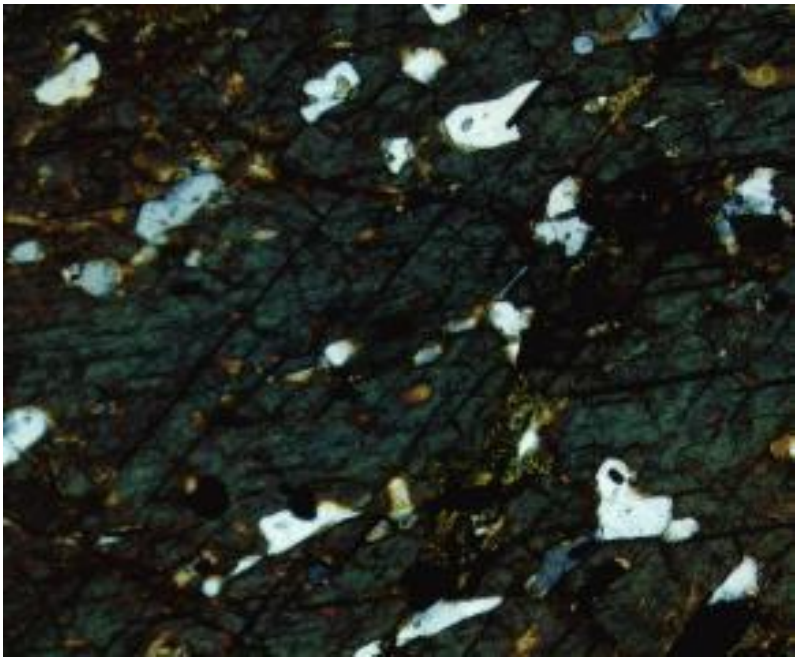

**Fig. 8.** Hornblende (dark green) with quartz sieve texture (white).

Chemical analyses of the La Quinta rocks (Table 1) indicate that the quartz diorite is metaluminous but becomes peraluminous as it grades to granodiorite and granite. Values of ACNK [mol. % $Al_2O_3$ divided by mol. % ($CaO + K_2O + Na_2O$)] range from 0.94 to 1.08. Rare-earth-element distribution patterns in the rocks and sphene are similar to those found by Sawka et al. (1984) except that the heavy rare-earth-elements tend to be a bit more abundant.

**Table 1. Chemical analyses in weight percent of oxides and parts per million of trace elements in sphene and in granite (Gr), granodiorite (Grd), and quartz diorite (Qd) from the La Quinta quartz diorite. Analyses by Chemex Labs Ltd. Values of A/CNK are also given.**

| Rock | Qd | Qd | Qd | Grd | Gr | Sphene |
|---|---|---|---|---|---|---|
| Sample No. | SRM-6 | SRM-4 | SRM-15 | SRM-2 | SRM-16 | crystals |
| wt.% | | | | | | |
| $SiO_2$ | 60.20 | 62.26 | 65.36 | 71.94 | 76.50 | -- |
| $TiO_2$ | 1.00 | 0.85 | 0.65 | 0.26 | 0.07 | -- |
| $Al_2O_3$ | 16.61 | 16.54 | 16.17 | 14.87 | 12.63 | -- |
| $Fe_2O_3$ (total Fe) | 6.77 | 5.61 | 4.60 | 1.97 | 0.92 | -- |
| MgO | 2.84 | 2.31 | 1.70 | 0.55 | 0.02 | -- |
| CaO | 5.38 | 5.17 | 4.25 | 3.18 | 1.10 | -- |
| $K_2O$ | 2.25 | 2.48 | 2.66 | 3.32 | 6.10 | -- |
| $Na_2O$ | 3.31 | 3.23 | 2.70 | 2.73 | 1.89 | -- |
| LOI | 0.77 | 0.80 | 0.84 | 0.47 | 0.22 | -- |
| total | 99.13 | 99.25 | 98.93 | 99.29 | 99.45 | |
| A/CNK | 0.94 | 0.95 | 1.07 | 1.07 | 1.08 | |
| ppm | | | | | | |
| La | 67 | 43 | 38 | 22 | 9 | 506 |
| Ce | 99 | 115 | 66 | 94 | 32 | 2000 |
| Nd | 17 | 14 | 2 | 23 | 12 | 737 |
| Sm | 6.0 | 7.0 | 6.0 | 2.0 | 1.0 | 565 |
| Eu | 1 | 1 | 1 | <1 | 1 | 101 |
| Tb | 1 | 1 | 1 | <1 | <1 | 53 |
| Yb | 4 | 3 | 3 | 1 | 2 | 141 |
| Lu | <1 | <1 | <1 | <1 | <1 | 26 |
| Rb | 100 | 92 | 94 | 90 | 170 | 16 |
| Sr | 350 | 420 | 350 | 430 | 230 | 185 |

## Discussion

By virtue of the gradual appearance of secondary K-feldspar and myrmekite, and the simultaneous parallel disappearance of plagioclase in the quartz diorite, this rock progressively changes into granodiorite and then to granite. Also, in early stages the association of hornblende containing quartz sieve textures with myrmekite lends support to the metasomatic origin of the granodiorite and granite (Collins, 1988; Hunt et al., 1992). The coexistence of the large sphene crystals with K-feldspar and myrmekite suggest the general immobility of titanium during the metasomatic processes that produced the K-feldspar. That is, where biotite breaks down and is replaced by quartz, released K, Ti, Fe, Mg, and Al are free to move to other sites. The K replaces some plagioclase crystals to form microcline and myrmekite, and in that process Ca, Na, and Al are released from the plagioclase (Collins, 1988; Hunt et al., 1992). Some of the released Ca and Al are precipitated as epidote overgrowths on allanite (Fig. 7). Because the Ti ion has a large charge of $4^+$, it does not travel far before it is precipitated with released Ca to form sphene. The rounded and embayed inclusions of plagioclase inside the sphene crystals suggest that the sphene has replaced the plagioclase in zones of cataclasis (Figs. 3 and 4). Some released Fe goes into magnetite, but much Fe, Mg, and Ca are carried out of the system.

Experimental studies by Moody et al. (1983) suggest that sphene is not stable above 500º C at 2-4 kbar, but other studies by Hunt and Kerrick (1977) extend the range to 580º C at 3-5 kbar. Above these temperatures ilmenite is the stable phase in which the Ti precipitates. Because myrmekite must also form at these same T-P conditions, the association of myrmekite and sphene supports the hypothesis that they are simultaneous metasomatic products rather than the sphene being a primary mineral that crystallized earlier from quartz diorite magma.

## Lyon Mountain granite gneiss, Ausable Forks, New York

### 1. *Regional relationships*.

The Lyon Mountain granite gneiss north of Ausable Forks, New York, occurs in the Clinton County magnetite district (Fig. 9) and is the host rock for 35 abandoned iron (magnetite) mines among which are the Palmer Hill mine (Fig. 10) and Jackson Hill mine (Fig. 11) (Collins, 1959, 1969; Hagner and Collins, 1967; Postel, 1952). The magnetite in the iron ore zones contains traces of sphene but is considered to be non-titaniferous, generally containing trace amounts to 1 wt. % $TiO_2$ with only local spotty values as high as 2.55 wt. % $TiO_2$ (Postel, 1952).

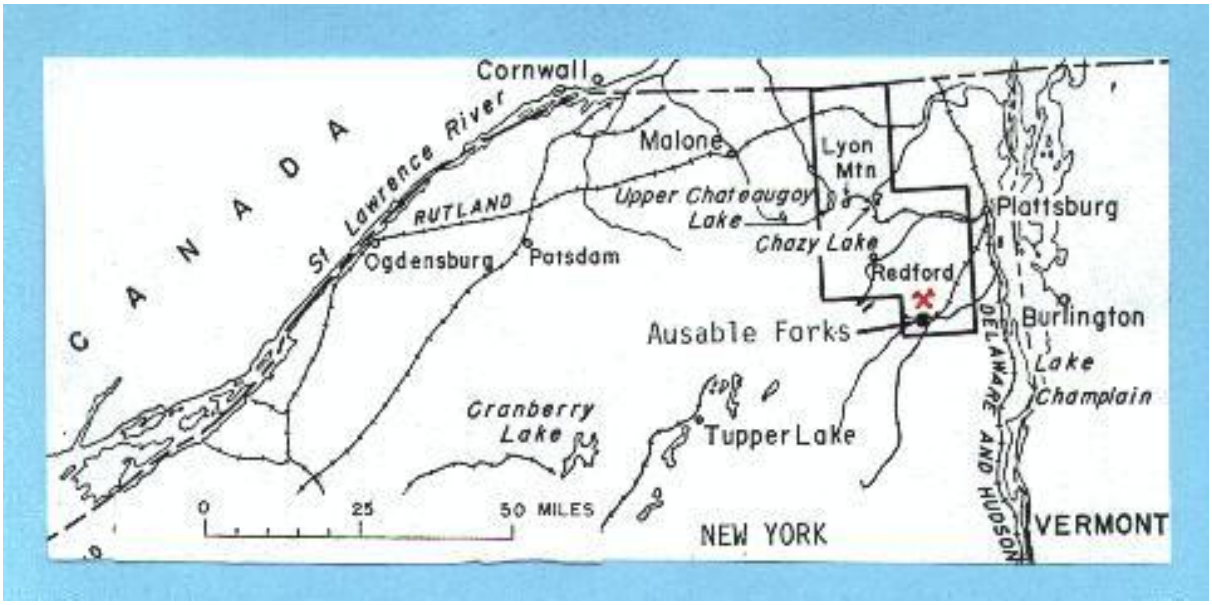


**Fig. 9.** Location of the Lyon Mountain granite gneiss in the Clinton County magnetite district, in northern New York, adjacent to the Canadian border and west of Vermont, is outline in black. Location of the Palmer Hill and Jackson Hill mines north of Ausable Forks is indicated by red mine symbol. Map is modified after Postel (1952)

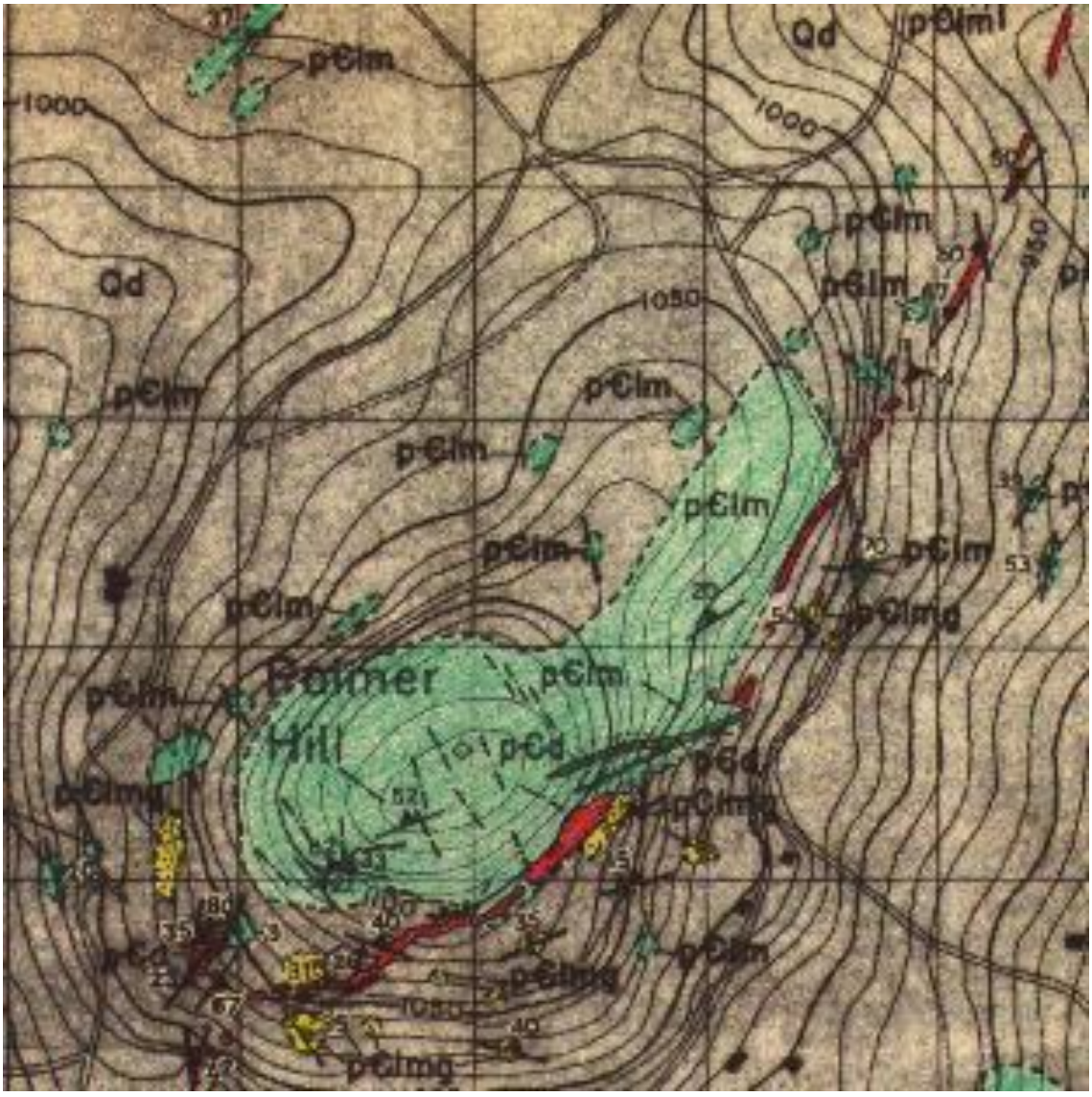


**Fig. 10.** Part of map, showing geology and structure of the Palmer Hill magnetite iron mine (Collins, 1959). Undifferentiated Lyon Mountain granite gneiss (green); garnet-bearing alaskite (yellow); and magnetite ore zones (red). The symbol dash-dot-dash indicates the location and strike of pegmatite dikes cutting the granite. Grid pattern is at 500-foot intervals (~150 m).

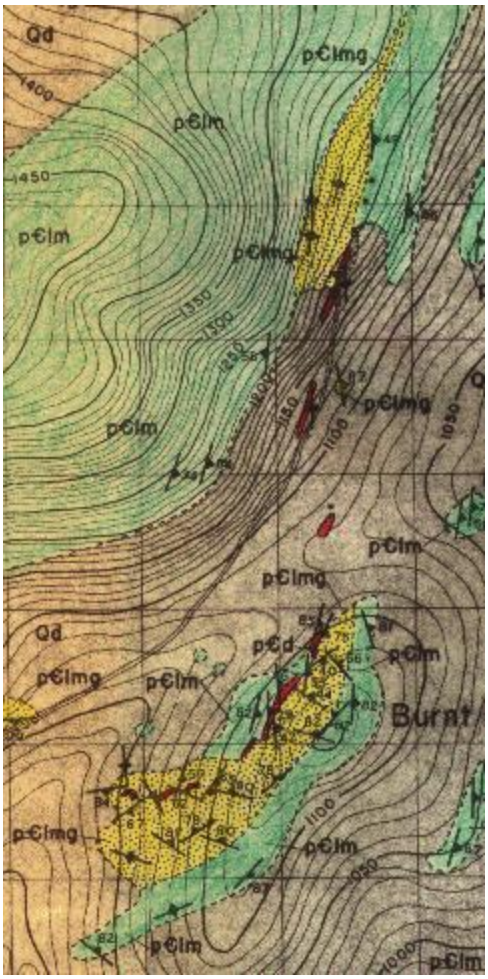


**Fig. 11.** Part of map, showing geology and structure of the North and South Jackson Hill magnetite iron mines on Burnt Hill and Bear Hill (Collins, 1959). Undifferentiated Lyon Mountain granite gneiss (green); garnet-bearing alaskite (yellow); and magnetite ore zones (red). Grid pattern is at 500-foot intervals (~150 m).

The host granite gneiss consists of four different facies in a continuum of dominant feldspar types (Fig. 12), ranging from microcline (Fig. 13) to perthite (with coarse plagioclase lamellae; Fig. 14 and Fig. 15) to antiperthite (Fig. 16) to plagioclase (not illustrated). In the microcline facies the microcline is slightly perthitic with primary, barely-visible, thin, exsolved, evenly-distributed, albite lamellae. In the perthite facies, some of the microcline crystals contain only primary, thin, albite lamellae, but other coexisting microcline crystals also contain secondary, thicker, plagioclase lamellae. These lamellae are unevenly-distributed and in many places are of unequal thicknesses. These secondary coarse plagioclase lamellae initially appear where the microcline crystals are deformed (Fig. 14) and

adjacent to a side where an albite rim first appears. In the antiperthite facies, the islands of K-feldspar are of unequal size and irregularly distributed (Fig. 16). In the plagioclase facies, isolated grains of antiperthite may occasionally be found.

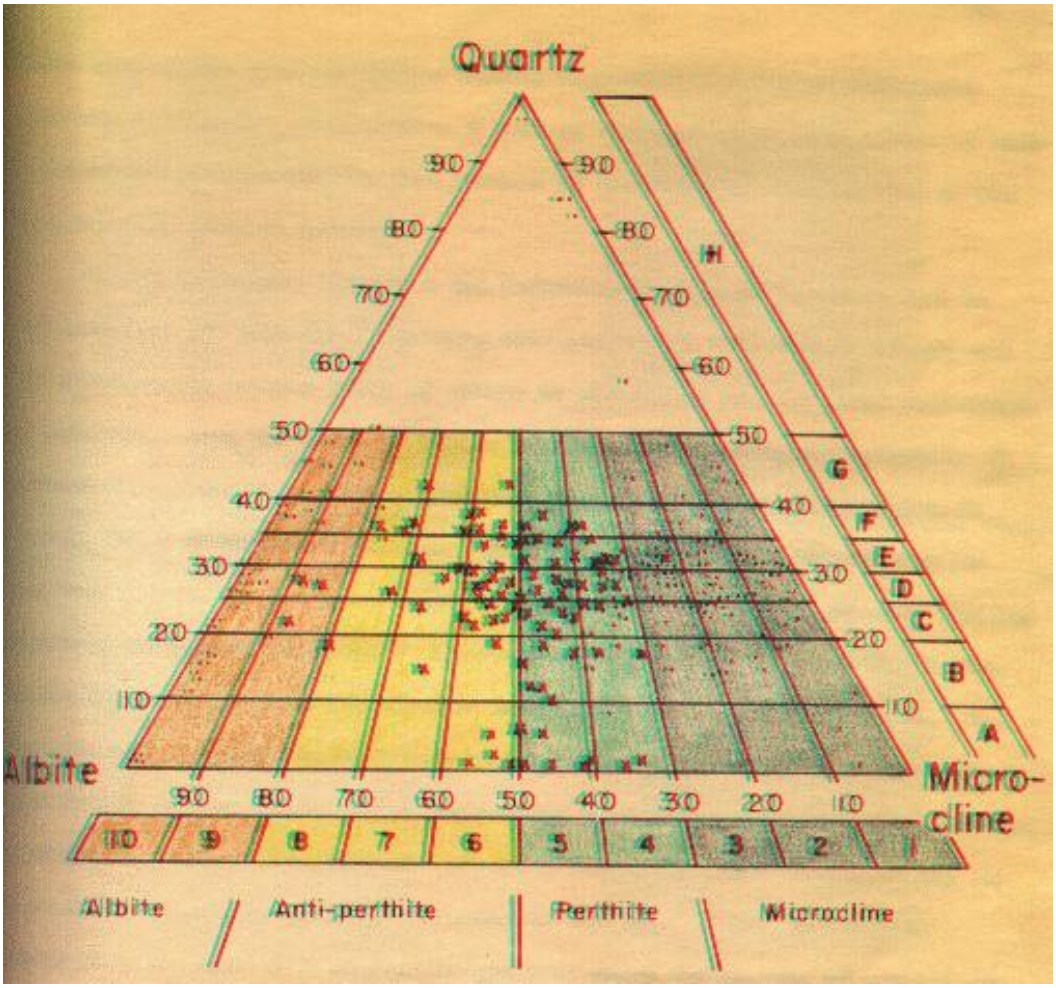


**Fig. 12.** Triangular diagram showing proportional modal percentages of quartz, plagioclase (albite-oligoclase), and K-feldspar (microcline) in the Lyon Mountain granite gneiss. Granite gneiss samples lacking antiperthite or perthite are indicated by dots, those containing antiperthite or perthite by x's.

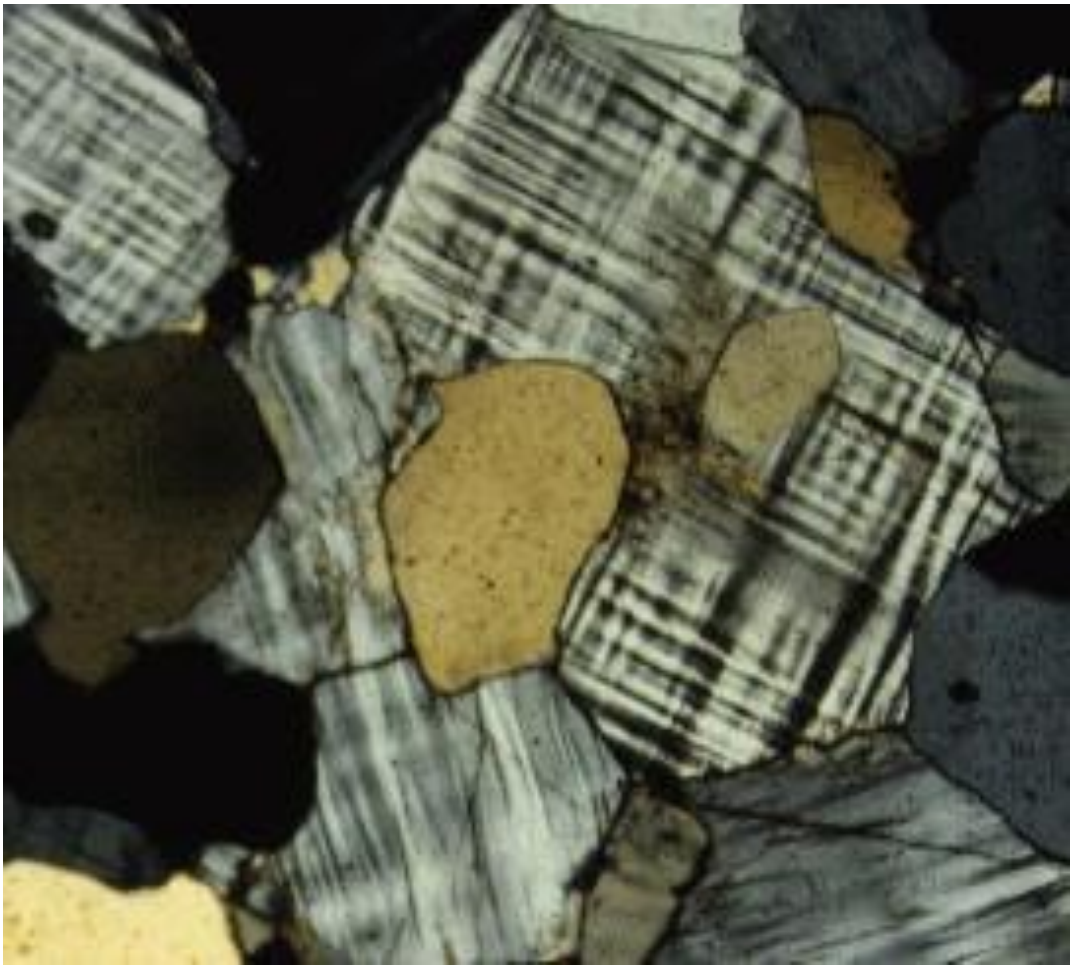

**Fig. 13.** Microcline clinopyroxene granite gneiss. Microcline (cross-hatch pattern, gray and white); quartz (clear, rounded crystals; white, gray, and cream); magnetite (black).

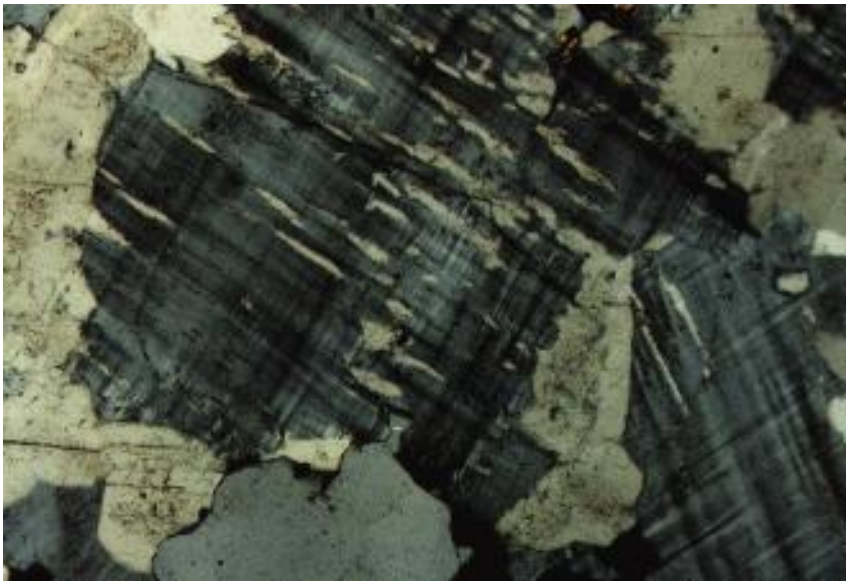

**Fig. 14.** Perthite with microcline (cross-hatch pattern; gray) and coarse, unevenly-distributed secondary plagioclase lamellae (cream). Plagioclase (cream) on border of the perthite is optically continuous with plagioclase lamellae. Quartz (rounded clear crystals, light gray).

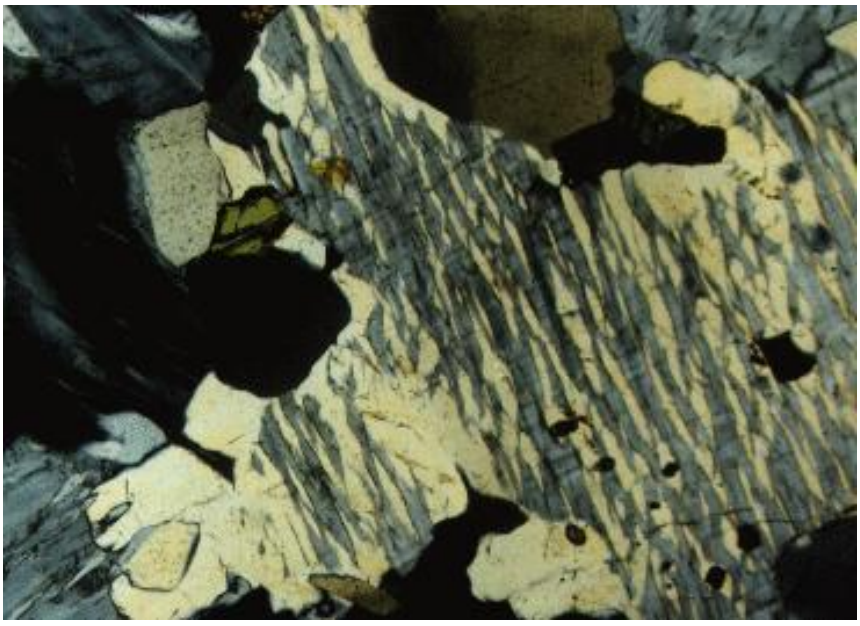

**Fig. 15.** Perthite with microcline (gray) and coarse, unevenly-distributed, secondary plagioclase lamellae (cream). Plagioclase (cream) on border of the perthite is optically continuous with plagioclase lamellae. Quartz (rounded clear crystals; dark cream, top), clinopyroxene (dark green); tiny magnetite crystals (black).

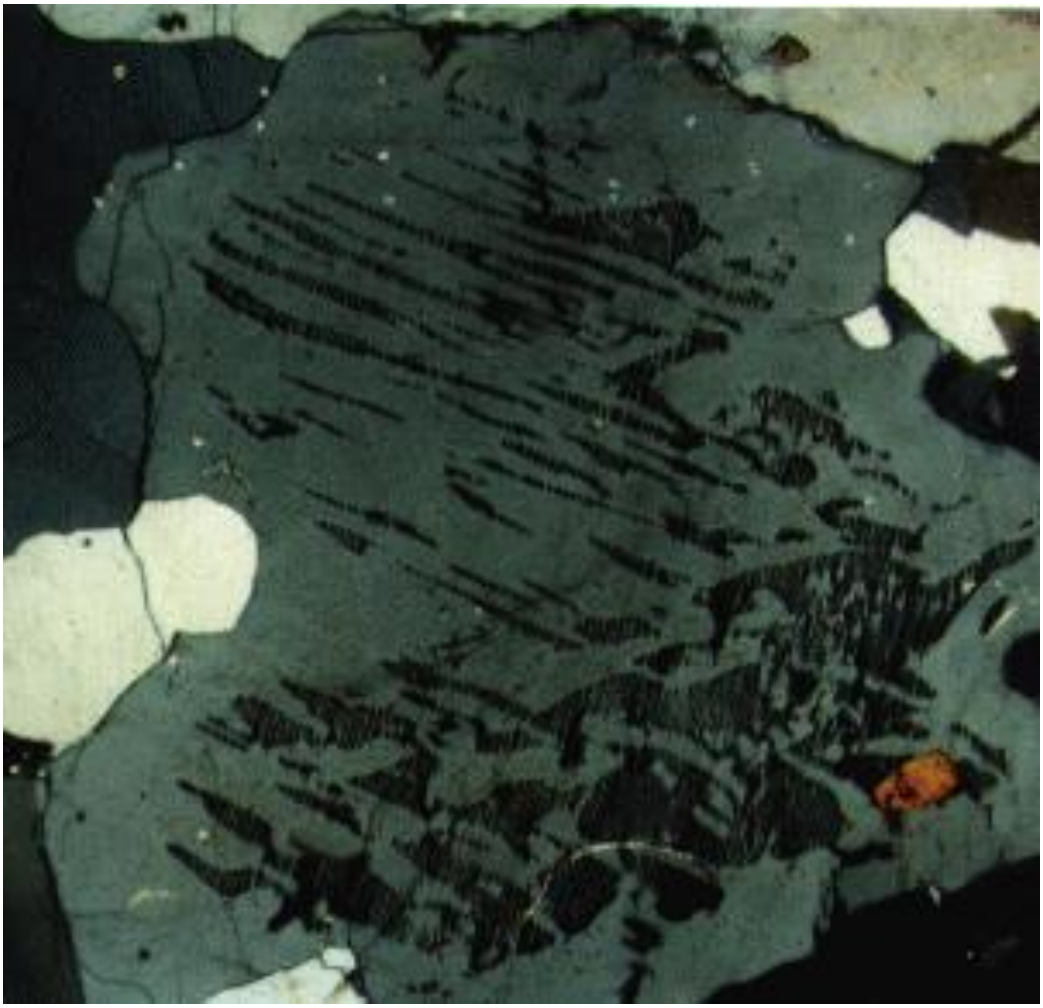

**Fig. 16.** Antiperthite with islands of K-feldspar (dark gray) in plagioclase (light gray). Quartz (rounded, clear crystals; white or cream); sphene (tiny, oval, tan).

Besides the feldspars, clinopyroxene (5-10 vol. %), quartz (0-50 vol. %), magnetite (0-7 vol. %), and sphene (0-7 vol. %) are the dominant coexisting minerals. The sphene occurs most abundantly as isolated, euhedral, rounded grains (Fig. 15 and Fig. 17), but it also occurs as narrow anhedral rims on magnetite (Fig. 18) and in a few places bordering garnet (Fig. 19). Apatite, zircon, and fluorite (rare) are accessories; chlorite is an alteration product of the ferromagnesian silicates. Locally, clinopyroxene-plagioclase or clinopyroxene-hornblende-plagioclase skarns occur in the granite gneiss and contain 35-80 vol. % clinopyroxene. In other places away from the iron mines, the Lyon Mountain granite gneiss contains hornblende (1-10 vol. %) and/or Mg-rich biotite (1-3 vol. %), but most Lyon Mountain granite gneiss contains clinopyroxene as the only ferromagnesian silicate. Magnetite occurs either as primary disseminated grains or as secondary replacements of fractured feldspars or clinopyroxene.

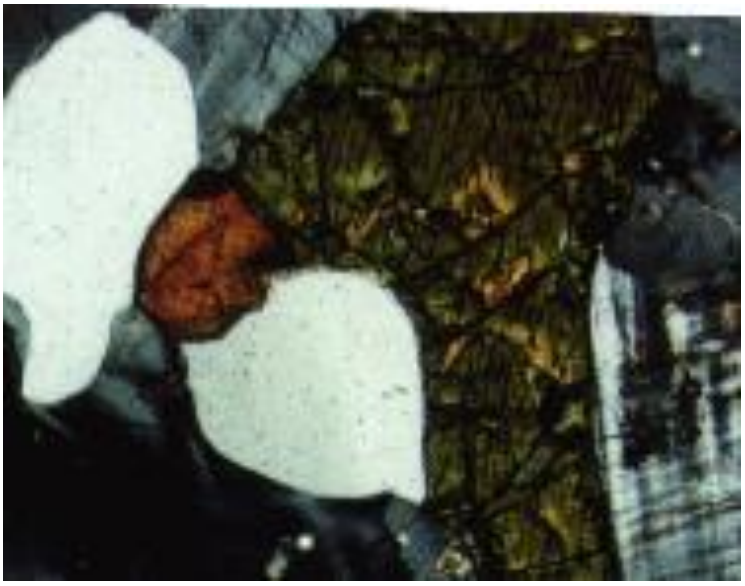

**Fig. 17.** Rounded isolated oval sphene grain (tan) adjacent to clinopyroxene (green); quartz (white); microcline (gray, black, and cross-hatch pattern).

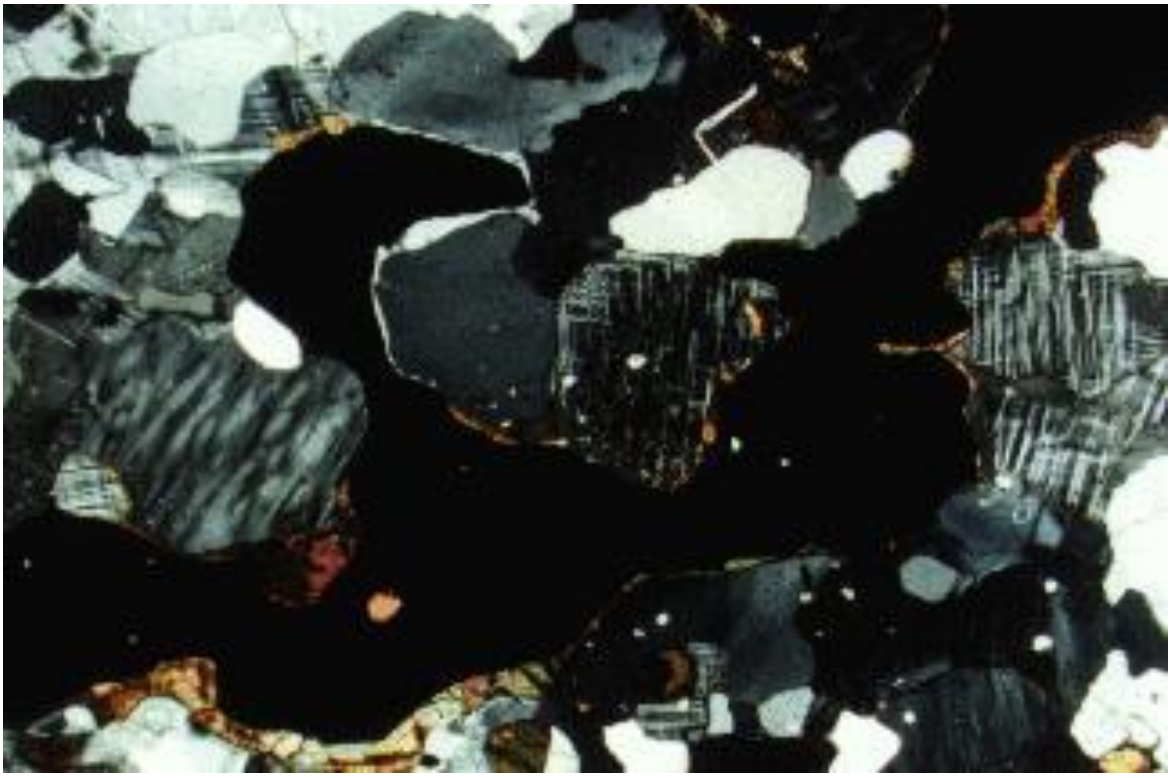

**Fig. 18.** Narrow, anhedral sphene rims (tan, brown) on magnetite (black). Quartz (rounded clear crystals, white, gray); microcline (cross-hatch pattern; gray and light gray).

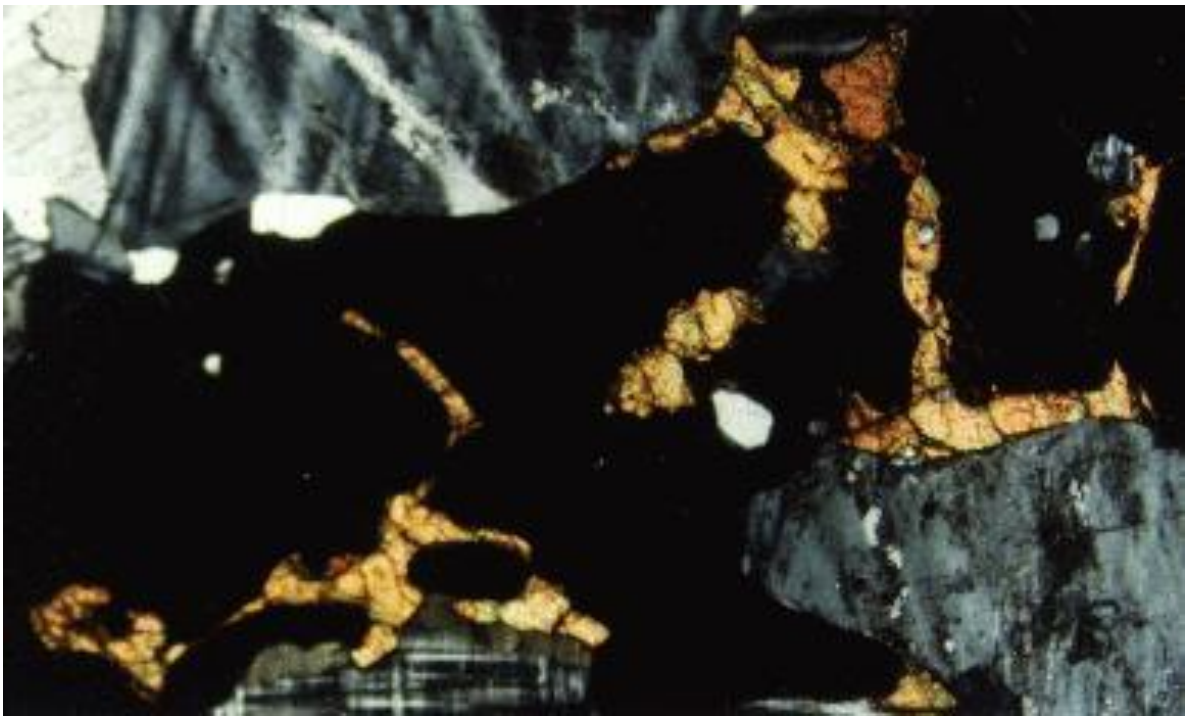

**Fig. 19.** Anhedral sphene rims (tan) on garnet (black); microcline (gray) surrounds the garnet.

On a regional basis modal sphene varies inversely with modal magnetite and tends to be highest near but not adjacent to the magnetite ore zones (Collins, 1959; Hagner and Collins, 1967). The association of magnetite and sphene near magnetite ore zones is not unexpected because Ti tends to be where Fe is present. Most sphene in the region is primary and formed at the same time that the disseminated magnetite was formed during granulite-grade metamorphism that produced the clinopyroxene-microcline gneiss, but some sphene is secondary near the ore zones and occurs as overgrowths on magnetite (Fig. 18) and garnet (Fig. 19). When all the magnetite and sphene data are plotted without regard to distance from the magnetite ore zones, modal sphene occurs only as trace amounts where coexisting magnetite is greater than 4.7 vol. % either far from or in the ore zones, but then rises to an average value of 1 vol. % as magnetite modal percentages decrease from 4.7 vol. % to zero (Fig. 20).

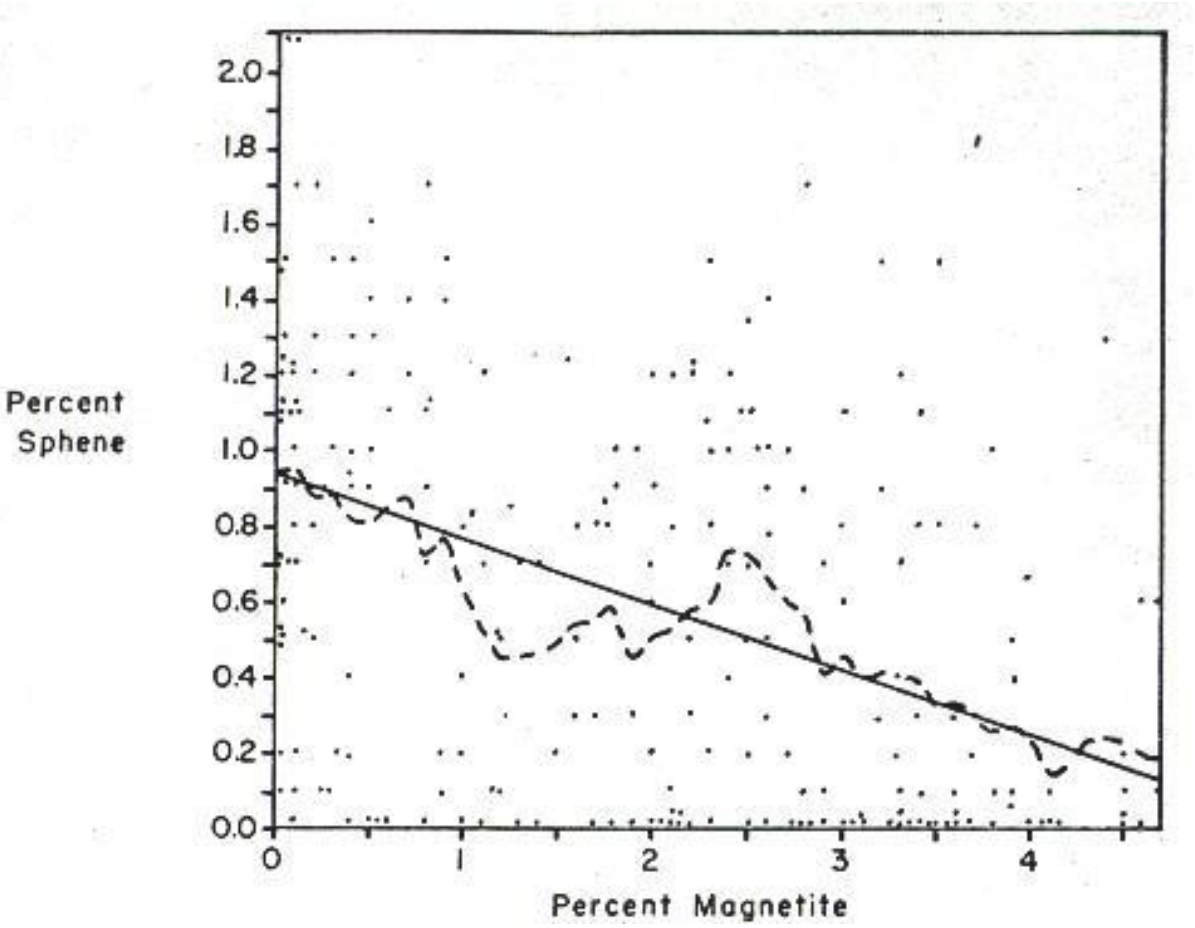


**Fig. 20.** Diagram showing modal sphene percentages plotted against modal magnetite percentages. Values of magnetite in the range of 4.7-55.0 vol. % are not shown, but average values of sphene approach zero and become asymptotic to the abscissa. Averaged values of sphene percentages are plotted along the dashed line; the trend is indicated by the solid line.

**2. *Magnetite ore zones and wall rocks*.**

Adjacent to the magnetite ore zones the four Lyon Mountain granite gneiss facies were modified by fluids which permitted the disseminated magnetite in the wall rocks to be concentrated in the ore zones. At distances greater than 150 m (~500 feet) away from the iron mines (Fig. 10 and Fig. 11), the clinopyroxene granite gneiss is relatively undeformed. Toward the ore zones, the granite gneiss exhibits increasing degrees of deformation and local brecciation (Collins, 1959; Hagner and Collins, 1967). In the 150-m transition to the iron ore zones the following four kinds of changes occur.

***(1)*** Tertiary albite plagioclase replaces microcline in the perthite facies so that the coarse secondary plagioclase lamellae of the perthitic microcline project into the tertiary plagioclase like teeth of a comb (Fig. 21 and Fig. 22). Where the tertiary plagioclase is oligoclase instead of albite, quartz blebs occur in the plagioclase to make it myrmekitic (Fig. 23, Fig. 24, Fig. 25, and Fig. 26).

**Fig. 21.** Replacement of K-feldspar (gray) in the perthite by tertiary plagioclase (albite-twinned albite; dark) leave secondary plagioclase lamellae (cream) of the perthite projecting into the tertiary plagioclase.

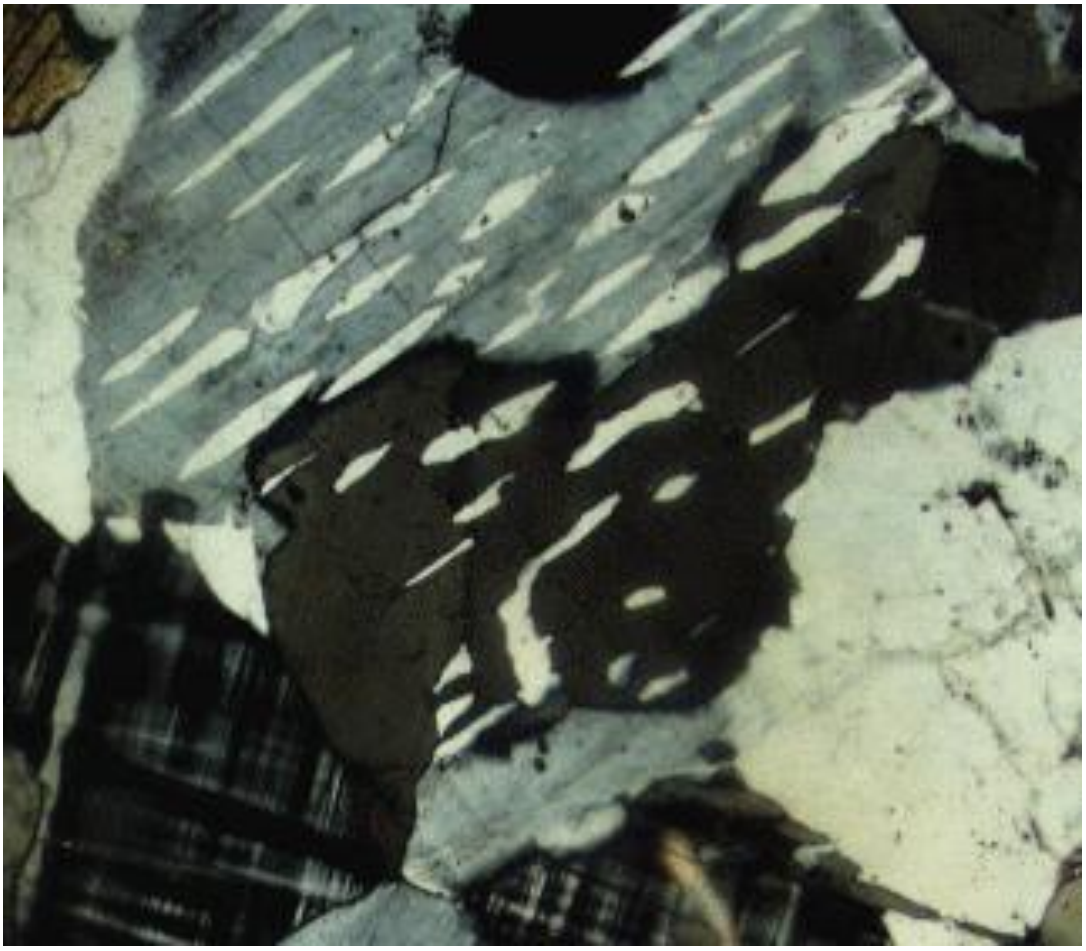

**Fig. 22.** Replacement of K-feldspar (gray) in perthite by tertiary plagioclase (albite-twinned albite; dark) leave secondary plagioclase lamellae (cream) of the former perthite as optically continuous islands in the tertiary plagioclase. Note adjacent plagioclase (cream white) also replaces K-feldspar in perthite (bottom right) with remnant plagioclase lamellae (tan) projecting into the plagioclase (cream white).

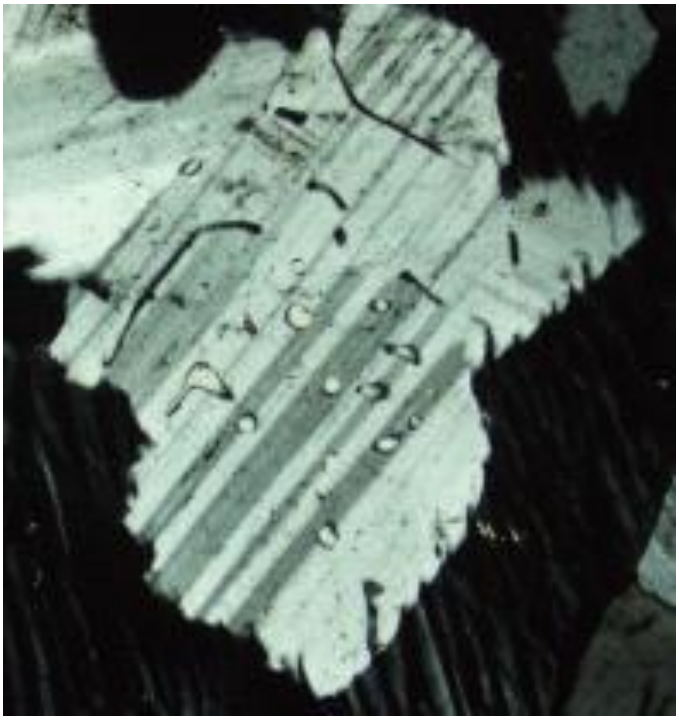

**Fig. 23.** Replacement of K-feldspar (black)) in perthite by tertiary albite-twinned oligoclase (cream and gray) leave secondary plagioclase lamellae (dark gray) of the perthite projecting into the tertiary plagioclase. The tertiary plagioclase contains scattered ovals and vermicules of quartz, and thus is myrmekitic.

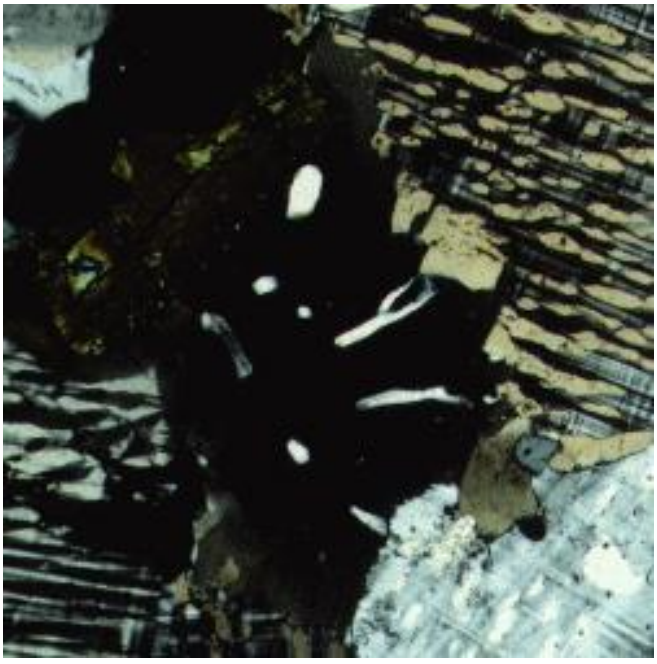

**Fig. 24.** Myrmekite replacing K-feldspar in perthite.

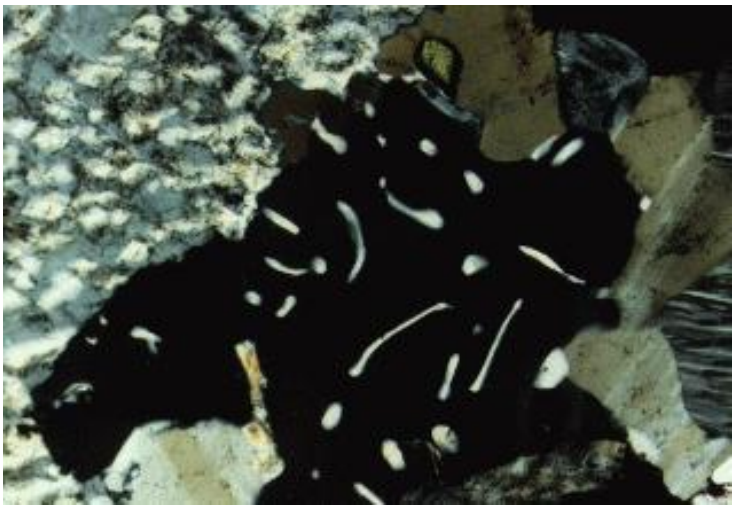

**Fig. 25.** Myrmekite replacing K-feldspar in perthite, showing isolated quartz vermicules of irregular shape.

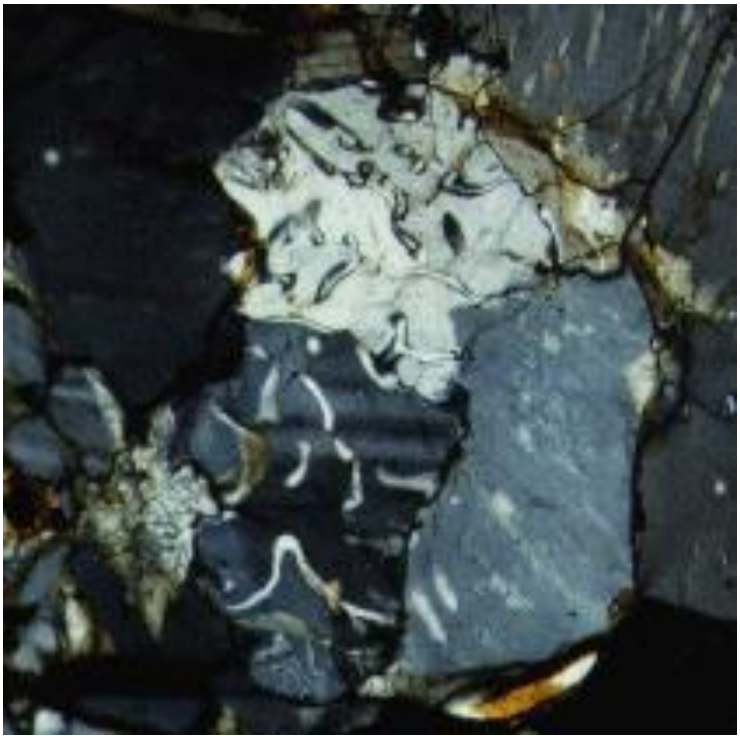

**Fig. 26.** Myrmekite replacing perthite.

*(2)* The clinopyroxene is locally replaced by magnetite (Fig. 27) or disappears; quartz increases from less than 30 vol. % to greater than 30 vol. %, and in some places more than 50 vol. %, and locally andradite garnet appears (Fig. 19). As clinopyroxene disappears and quartz increases, the proportions of residual feldspars increase so that the gneiss is converted into a felsic alaskite, consisting

almost entirely of quartz and feldspars but containing trace amounts to 5 vol. % andradite garnet in some places.

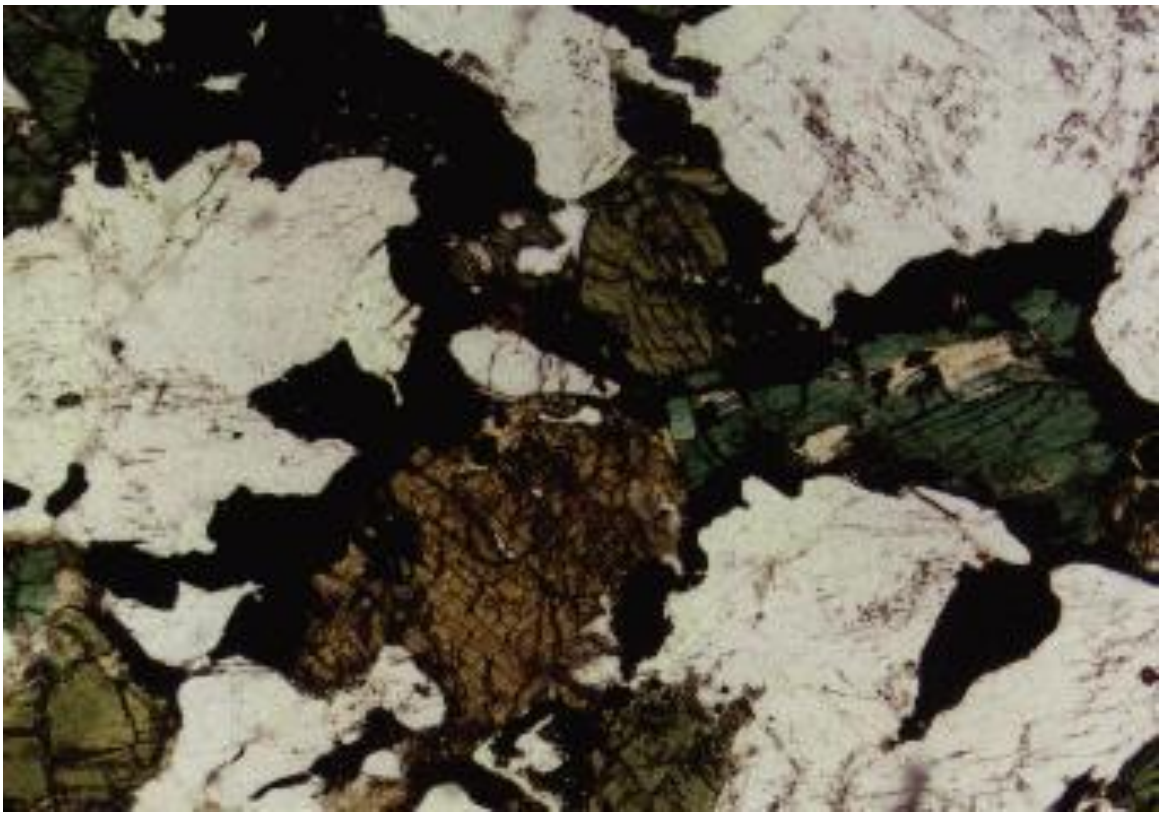

**Fig. 27.** In plain light, clinopyroxene (green, brown) replaced by magnetite (black). Some magnetite replaces feldspars along fractures.

***(3)*** Modal magnetite (4 to 7 vol. %) decreases gradually and then disappears before increasing abruptly to 50-100 vol. % in the ore zones. The degree of subtraction of magnetite from the wall rocks and width of subtraction may differ on opposite sides of the ore zones and are functions of the degree and width of deformation of the rocks and their conversion to alaskite (e.g., Fig. 11 and Fig. 28).

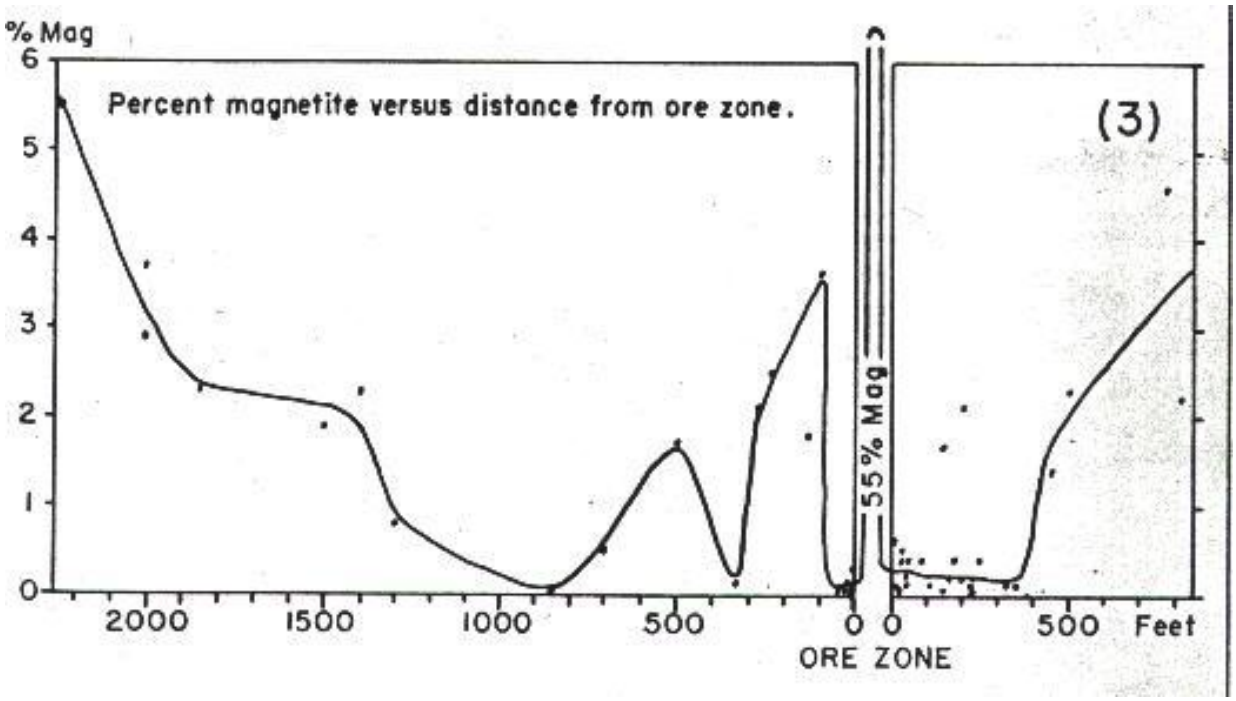


**Fig. 28.** Diagram of modal magnetite percentages plotted as a function of distance from the magnetite ore zones at the South Jackson Hill mine.

*(4)* Modal sphene, both primary and secondary, disappear except where garnet occurs, and then traces of sphene may remain (Collins, 1959; Hagner and Collins, 1967).

**3. *Chemical studies*.**

Spectrographic analyses of the ferromagnesian silicates and composite rock samples (Table 2) were done in order to compare distributions of major and trace elements. These analyses were done in 1958 and will be used *only for qualitative comparisons* because some values of analyzed oxides sum to totals less than 90 wt. % and $K_2O$ was not determined (Hagner and Collins, 1967). Nevertheless, comparisons between mineral and rock samples on a relative basis are reasonable approximations. Most clinopyroxene in the gneisses is iron-rich hedenbergite (e.g., sample number 128, Table 2), but in a few places the clinopyroxene has intermediate Fe contents (e.g., sample numbers 345 and 26). Hornblende is less Fe-rich than the clinopyroxene, and biotite is relatively Mg-rich. The andradite garnet is Fe-rich and Mg-poor, like the hedenbergite clinopyroxene, but contains proportionally more Ca and Al and less Si.

Table 2. Spectrographic analyses in weight percent of oxides in garnet (gar), clinopyroxene (cpx), hornblende (hbl), and biotite (bio) and in composite samples (40 each) of the Lyon Mountain clinopyroxene granite (gra) at distances less than 150 m (500 feet) from the ore zone and more than 150 m (500 feet) from the ore zone. Analyses were done by Oiva Joensu (Collins, 1959).

| No. | gar 61 | cpx 128 | cpx 345 | cpx 26 | hbl 345 | hbl 164 | bio 164 | bio 96 | gra -150 | gra +150 |
|---|---|---|---|---|---|---|---|---|---|---|
| wt.% | | | | | | | | | | |
| $SiO_2$ | 38 | 48 | 50 | 50 | 45 | 44 | 40 | 40 | 69 | 64 |
| $TiO_2$ | 0.3 | 0.15 | 0.15 | 0.12 | 0.33 | 0.75 | 1.50 | 0.95 | 0.43 | 0.7 |
| $Al_2O_3$ | 4.2 | 2.6 | 2.2 | 2.1 | 7.2 | 6.6 | 11.5 | 12.0 | 14.0 | 15.0 |
| Fe | 19 | 19.5 | 10.5 | 9.5 | 12.0 | 11.5 | 8.5 | 7.7 | 2.5 | 4.3 |
| MnO | 0.42 | 0.25 | 0.22 | 0.25 | 0.25 | 0.15 | 0.08 | 0.13 | 0.02 | 0.03 |
| MgO | 0.48 | 1.5 | 9.0 | 10.0 | 12.5 | 13.0 | 17.5 | 20.0 | 0.36 | 0.80 |
| CaO | 32 | 23 | 22 | 23 | 9.7 | 9.5 | 0.5 | 0.2 | 1.6 | 1.5 |
| $K_2O$ | — | — | — | — | — | — | — | — | — | — |
| $Na_2O$ | 0.2 | 2.0 | 2.5 | 2.1 | 2.5 | 2.5 | 0.2 | 0.2 | 4.5 | 5.0 |
| total | 94.60 | 97.00 | 96.57 | 97.07 | 89.48 | 88.00 | 79.78 | 81.18 | 92.41 | 86.33 |
| ppm | | | | | | | | | | |
| $Cr_2O_3$ | 35 | 40 | x | x | 35 | 110 | 50 | x | 25 | 280 |
| $V_2O_3$ | x | x | x | x | x | 130 | 90 | x | x | 55 |
| $Sc_2O_3$ | 100 | 65 | 30 | 60 | 60 | 90 | 30 | 200 | 15 | 50 |
| $Y_2O_3$ | 1800 | 120 | 140 | 110 | 160 | 420 | 35 | 30 | 200 | 160 |
| $Yb_2O_3$ | 160 | 15 | 15 | 10 | 18 | 35 | x | x | 22 | 15 |
| $Be_2O_3$ | x | 200 | 200 | 200 | x | 100 | x | x | x | x |
| $La_2O_3$ | 70 | x | x | x | 65 | 80 | x | x | x | x |
| CoO | x | 150 | 75 | 30 | 65 | 25 | 40 | 55 | 4 | x |
| NiO | x | 8 | x | 8 | x | 90 | 125 | 15 | 50 | 30 |
| CuO | 60 | 30 | 20 | 15 | 20 | 25 | 30 | 120 | 10 | 15 |
| $ZrO_2$ | 950 | 1000 | 850 | 1100 | 750 | 350 | 130 | 120 | 1200 | 1300 |

A composite of 40 samples typical of the wall rock at distances less than 150 m (~500 feet) away from the ore zones contains 2.5 wt. % Fe and 0.43 wt. % $TiO_2$. whereas a composite of 40 samples typical of the wall rock more than 150 m (~500 feet) away from the ore zones contains 4.2 wt. % Fe and 0.70 wt. % $TiO_2$ (Table 2).

The spectrographic analyses of the composite samples show that Ti, Al, Fe, Mn, Mg, Na, Cr, V, Zr, Sc, and Cu decrease in the gneisses near the ore zones and that Si, Ca, Co, Ni, Y, and Yb increase. The elements that decrease were removed from the wall rocks by escaping fluids. The elements that increase were concentrated in residual minerals. The greater amounts of Si can be explained by the increased modal percentages of quartz and feldspars relative to the disappearance of the ferromagnesian silicates, sphene, and magnetite. The increase in Co, Ni, Ca, Y, and Yb is explained by the concentration of these elements in residual magnetite, sphene, and andradite garnet.

## Discussion

### 1. *Na- and Ca-metasomatism, first stage*.

The thin sections show that the perthite and antiperthite facies are the result of Na-metasomatism of deformed microcline crystals, which produced much thicker plagioclase lamellae and veins than the thin, exsolved lamellae in the original microcline crystals. If the thick plagioclase lamellae had formed by exsolution from high-temperature K-feldspar crystallized from magma, then all K-feldspar crystals in a given sample should contain plagioclase lamellae of similar thicknesses and in a uniform distribution, and this is not the case. During Na-metasomatism, the sodic plagioclase (albite) was first formed by penetration of Na along crystal boundaries replacing rims of the K-feldspar (Fig. 29), then penetrated along fractures part way into the crystal (Fig. 30 and Fig. 31), and finally extended completely through the crystals to form coarse lamellae in perthite (Fig. 32 and Fig. 33). In some places the replacement of the K-feldspar by albite was so extensive that only remnants of the K-feldspar remained, resulting in antiperthite (Fig. 34 and Fig. 35). The antiperthite facies is gradational to the plagioclase facies in which only a few crystals in a thin section have remnants of K-feldspar. Therefore, presumably, some plagioclase facies, lacking K-feldspar remnants, are places where the first of two stages of Na-metasomatism has completely replaced former K-feldspar crystals.

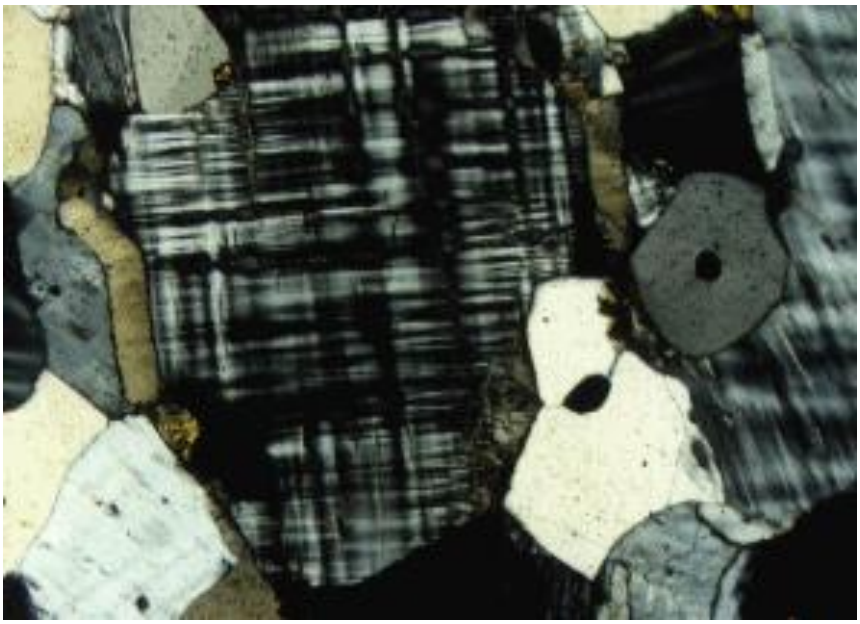

**Fig. 29.** Narrow rims of plagioclase (albite; dusky cream) replace left and right borders of K-feldspar (cross-hatch pattern, black and white). Quartz (rounded clear crystals; white, cream, gray).

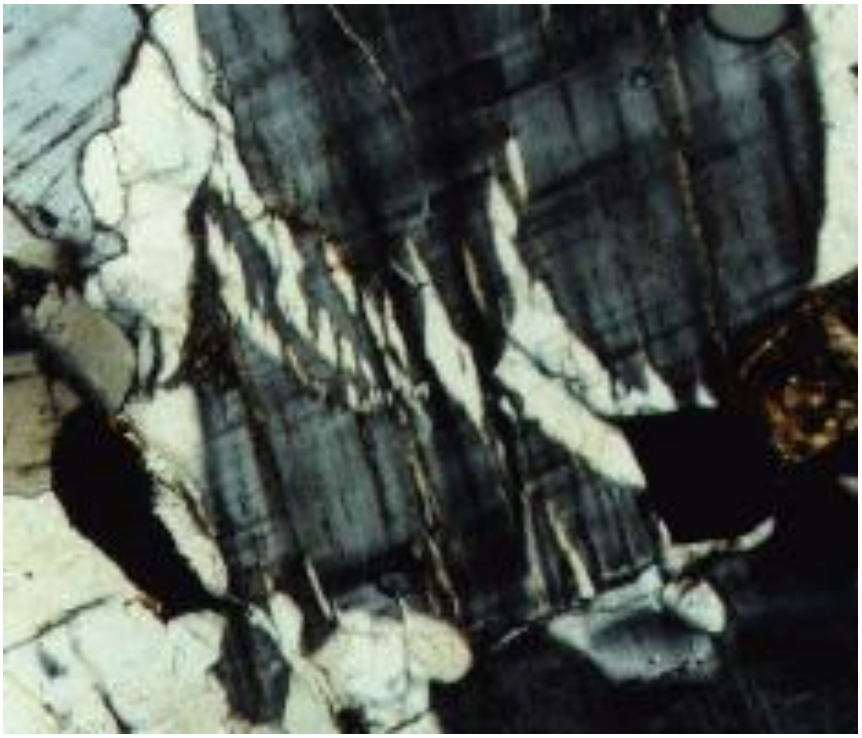

**Fig. 30.** Fractured microcline (cross-hatch pattern, gray) with early stage of formation of secondary albite plagioclase lamellae (cream white), penetrating the microcline.

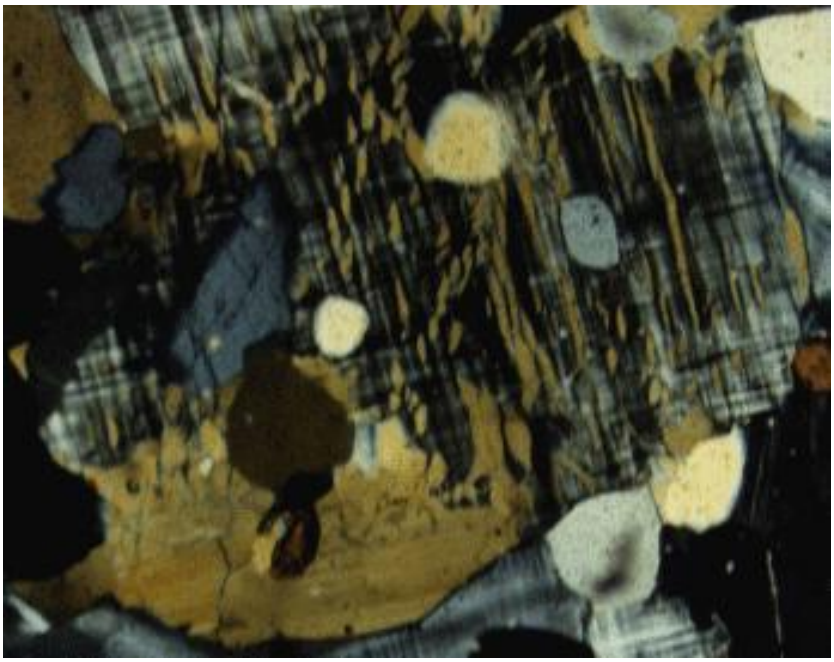

**Fig. 31.** More advanced stage of replacement of microcline (gray) to produce albite lamellae (dark cream). The plagioclase has completely replaced the microcline in the lower part. Rounded clear grains are quartz.

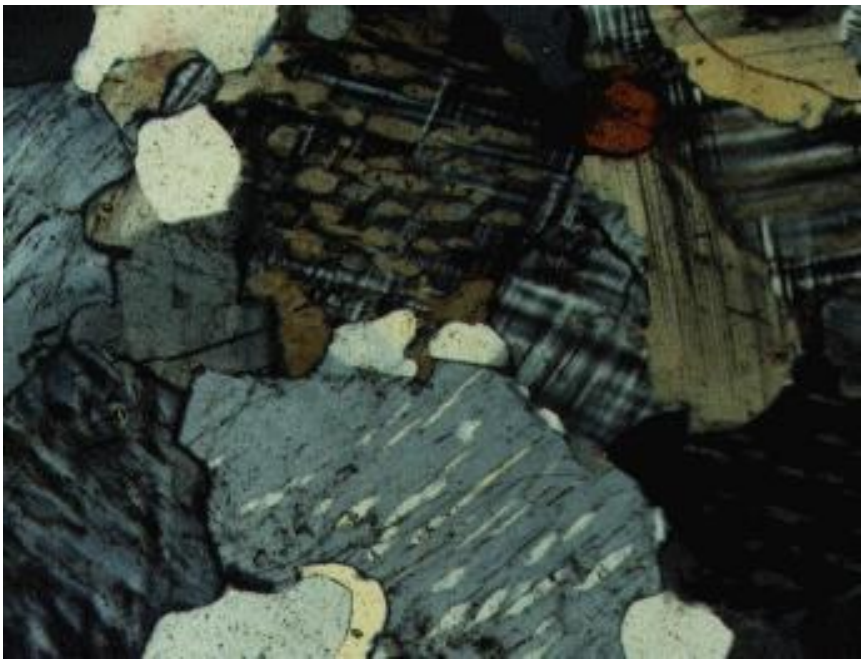

**Fig. 32.** Another advanced stage of replacement of microcline (gray) to produce secondary albite lamellae (cream and dark cream). Some microcline grains lack lamellae; some contain narrow lamellae; and some contain coarse thick lamellae. Rounded clear grains are quartz. Circular tan grain is sphene.

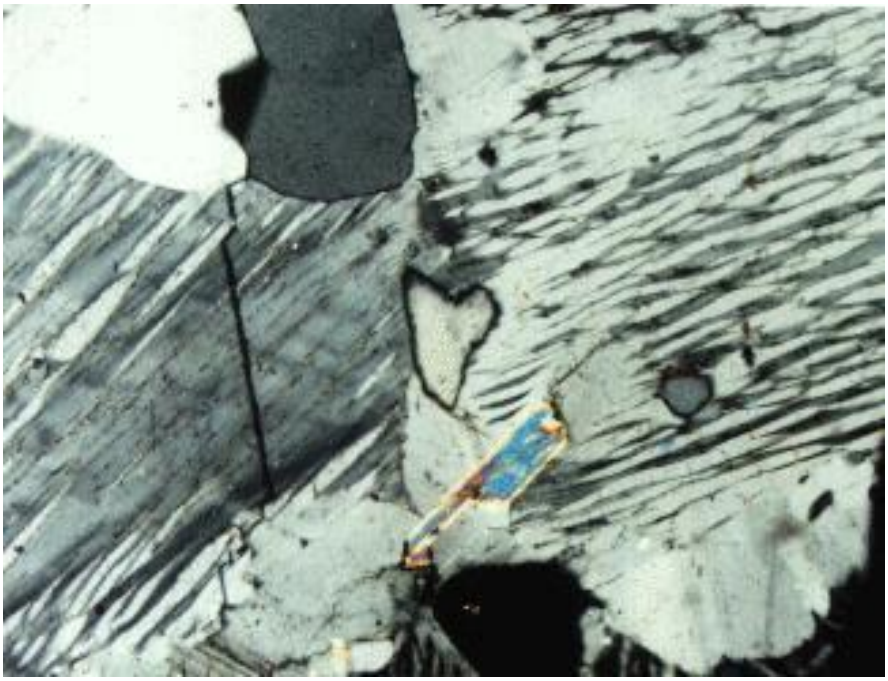

**Fig. 33.** Replacement of K-feldspar (gray) by secondary plagioclase exceeds 50 vol. % in right side so that the crystal here is antiperthite. On left side a portion of the microcline remains unreplaced. Quartz (rounded clear crystals; cream, gray, black), biotite (blue-green).

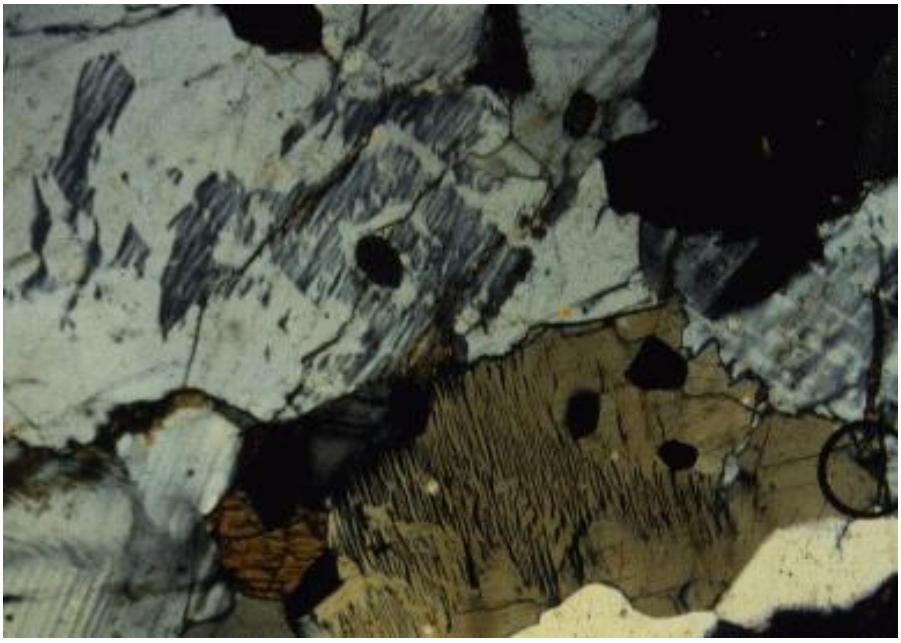

**Fig. 34.** Antiperthite with remnant K-feldspar (gray) in albite plagioclase (light cream; tan). Clinopyroxene (brown); sphene (dark oval grains); magnetite (angular black).

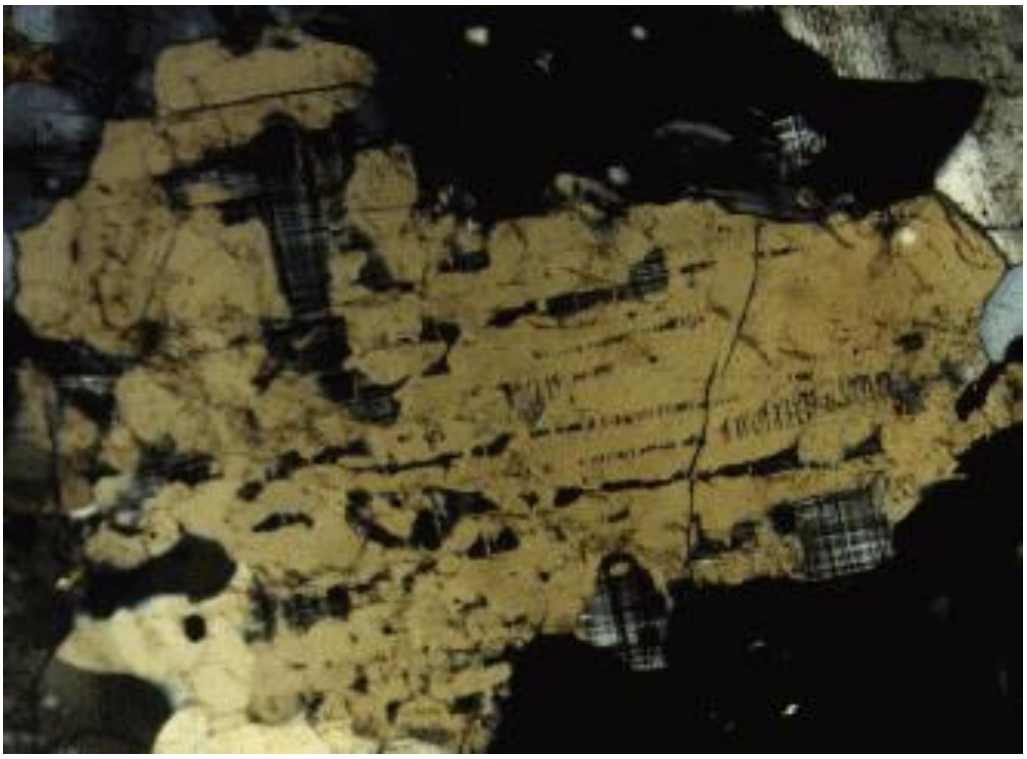

**Fig. 35.** Antiperthite with remnant K-feldspar (gray) in albite plagioclase (dark cream, tan). In other parts of the thin section, large plagioclase crystals lack any K-feldspar inclusions. Therefore, this picture illustrates the transition to the plagioclase granite gneiss facies.

The Lyon Mountain clinopyroxene granite gneiss is exposed in a 425 square kilometer area (164 square miles; Whitney and Olmsted, 1988). In this area the four feldspar gneiss facies (Fig. 12) have regional abundances that fall between the ranges of 5-11% for microcline gneiss, 36-55% for perthite gneiss, 18-29% for antiperthite gneiss, and 22-24% for plagioclase gneiss (Postel, 1952). On that basis, the volumes of granite gneiss in the 425 square kilometers that have been affected by Na-metasomatism to produce perthite, antiperthite, and plagioclase facies could be as much as 89 % (378 square kilometers), which is certainly large-scale metasomatism. Therefore, much K has been displaced by the Na and moved out of the system.

**2. *Na- and Ca-metasomatism, second stage*.**

A second stage of Na- and Ca-metasomatism occurred in this 425 square kilometers when renewed local deformation along limbs of anticlinal and synclinal folds created cataclastic shear zones where fluids carried Na and Ca to form new albite-oligoclase crystals that replaced K-feldspar in perthite, resulting in

myrmekite in some places. Unlike other terranes where K-feldspar-bearing alaskite and granite are formed by metasomatic processes, wartlike myrmekite with tapering and branched quartz vermicules is absent. This absence occurs because the K-feldspar in the Lyon Mountain granite gneiss is entirely primary rather than secondary. Because biotite and muscovite are generally absent in rocks subjected to granulite-grade metamorphism, there is no K-bearing mica which can break down in the deformed rocks and release K that would produce more K-feldspar and myrmekite by K-metasomatism of the plagioclase. Instead, K-feldspar in perthite and non-perthitic microcline are replaced by plagioclase during Na-metasomatism or Na- and Ca-metasomatism. During Na-metasomatism, introduced Na substitutes directly for K in K-feldspar, and, therefore, no excess silica is released to form quartz vermicules in myrmekite (Fig. 21 and Fig. 22). However, where both Na- and Ca-metasomatism occur, the plagioclase replacing the K-feldspar is a bit more calcic, and excess silica is left over to form quartz vermicules and thereby produces myrmekite. The quartz vermicules, however, do not extend to the edge of the plagioclase crystal toward the K-feldspar (as in K-metasomatism) but are scattered in the interior and form irregular spindles, arcuate patterns, and ovals inside the plagioclase (e.g., Fig. 25).

See Whitney and Olmsted (1988) for an alternative interpretation for the origin of the albite gneisses, suggesting that they are metavolcanic and metasedimentary rocks.

**3. *Andradite garnet*.**

Where slightly aluminous hedenbergite (Table 2) was recrystallized, some Ca, Fe, and Al were concentrated to form andradite garnet of smaller volume than in the original hedenbergite. In that process the garnet requires less silica in its structure than the clinopyroxene, and, therefore, some silica was left over to form quartz, either as tiny inclusions in the garnet or as separate crystals, increasing the modal percentage of quartz in the rock.

**4. *Sphene*.**

Titanium, which is released from replaced clinopyroxene, hornblende, and biotite (Table 2) and/or from dissolved ilmenitic magnetite, combines with released Ca to form secondary sphene rims on the magnetite (Fig. 18) and/or in a few places on garnet (Fig. 19). This deposition of released Ti in sphene indicates the relative immobility of Ti in this terrane in contrast to released Mg and other elements more soluble than Ti, which must have escaped the system. Nevertheless, although Ti is

one of the least mobile elements, the field and thin section evidence show that Ti is readily mobile because of the irregular but progressive disappearance of magnetite, clinopyroxene, and both primary and secondary sphene in the 150 m (~500 feet) interval on either side of the ore zones. The loss of Ti is also shown by the presence of 0.70 wt. % $TiO_2$ in rocks greater than 150 m from the ore zones and by only 0.43 wt. % $TiO_2$ in rocks closer to the ore zones (Table 2).

**5. *Magnetite*.**

The same fluids that caused a second stage of Na- and Ca-metasomatism dissolved Fe from disseminated magnetite in the deformed gneiss wall rocks and transported it to the relatively low-pressure sites in the shear zones where it was re-precipitated in magnetite concentrations (ore zones, 2-10 m wide). The magnetite replaced broken feldspar crystals (of all feldspar gneiss facies) and, thus, is clearly later than the first stage of Na- and Ca-metasomatism that produced the perthite and antiperthite. As the Fe in the magnetite was being dissolved and transported to the ore zones, some of the clinopyroxene in the granite gneiss was replaced by quartz and locally by garnet (trace to 5 vol. %). These replacements of the ferromagnesian silicates released additional Fe that also moved to the magnetite concentrations in the ore zones. The recrystallized and replaced rock became alaskite consisting mostly of quartz (greater than 30 vol. %) and feldspars, but in some places, also minor amounts of andradite garnet.

If an average of 2 vol. % magnetite were removed from 150 m (~500 feet) of wall rock on both sides of a low-pressure site in a central shear zone, then this magnetite could be deposited to form 6 m (20 feet) of pure magnetite. If the 19.5 wt. % Fe in 5-10 vol. % clinopyroxene (Table 2) that was replaced by quartz in alaskite in that same interval were transported and deposited in magnetite in the ore zones, then additional thickness of pure magnetite could be formed. Because the ore zone average about 10 m wide and only 50% magnetite, Fe removed from magnetite and clinopyroxene in the wall rocks is more than adequate to account for the magnetite concentrations.

Previous interpretations for the origin of the magnetite concentrations included suggestions that they were (1) metamorphosed sedimentary iron deposits, (2) magmatic segregations of residual Fe-rich fluids in granite magma, or (3) metasomatic deposits derived from pneumatolytic fluids expelled from granite magmas (Postel, 1952). The latter was the favored hypothesis in the early 1950s. There is no evidence of sedimentary structures or rock types that would support a sedimentary origin, and, therefore, this hypothesis was ruled out. If either of the

other two hypotheses were correct that the Fe concentrations resulted from magmatic segregation or that the Fe was brought in from outside sources by magmatic fluids, then amounts of magnetite in the wall rocks would be expected to be high near the ore zones and decrease gradually at increasing distances from the ore zones as the introduced Fe-rich fluids penetrated the wall rocks. Instead, the reverse patterns of zero amounts of magnetite in the adjacent wall rocks and increasing amounts with greater distances away from the ore zones give strong evidence that the Fe was derived from the wall rocks and not from distance magmatic sources.

Because more than enough Fe has been removed from the wall rocks to account for the magnetite concentrations in the ore zones, much Fe has also been carried away in escaping fluids. Large amounts of removed Ca, Mg, and Al, as well as other trace metals, are also unaccounted for. Small percentages of fluorite, green-and-pink fluoro-apatite, and sphene in the ore zones account for some of the missing Ca and suggest that HF may have been a catalyst to help transport the metals. A regional study of the terrane across several km beyond the iron mines shows that wherever the granite gneiss is cataclastically deformed, similar losses of Fe from magnetite and clinopyroxene and similar Na- and Ca-metasomatism of the K-feldspar took place, but in these deformed areas the appropriate low-pressure sites (shear zones) into which the Fe could be precipitated in magnetite were likely at higher levels and have been eroded away (Collins, 1959; Hagner and Collins, 1967).

## Conclusion

In both the La Quinta quartz diorite and the Lyon Mountain granite gneiss, the relative immobility of Ti in metasomatic terranes in comparison to other elements is demonstrated. Nevertheless, even Ti becomes mobile in final stages of metasomatism. In both terranes volumes of rock that are affected by metasomatic fluids occur across many square kilometers, if not hundreds of square kilometers. Therefore, the suggestion that plutonic rocks cannot be modified by large-scale metasomatism to produce granite and alaskite is shown to be false. If Ti can be moved in large volumes by metasomatic fluids, albeit late stages, then other elements of greater mobility can surely be moved as well during early stages. *The large volumes of K ions removed from the K-feldspar by Na-metasomatism to form albite in the Lyon Mountain granite gneiss must go somewhere and cause large-scale K-metasomatism at higher levels in the earth's crust*. If Na-metasomatism can modify 378 square kilometers of granite gneiss in New York, then K, whose

ionic charge of $1^+$ is the same as that of the Na ion and whose chemistry is similar, can surely be involved in large-scale K-metasomatism in other terranes.

Because sphene is stable in the range of 350-500º C and perhaps as high as 580º C (Moody et al., 1983; Sawka et al., 1984), which is below the melting interval for most granitic rocks, the possibility exists that sphene in some rocks is a clue that metasomatic fluids have moved through them. *The sphene could be an indication that both Ti and Ca have been released from minerals being modified by metasomatism*.

**References**

Collins, L. G., 1959, Geology of the magnetite deposits and associated gneisses near Ausable Forks, New York: unpublished Ph.D thesis, University of Illinois, 147 p.

Collins, L. G., 1969, Host rock origin of magnetite in pyroxene skarn and gneiss and its relation to alaskite and hornblende granite: Economic Geology, v. 64, p. 191-201.

Geyer, B. L., 1962, Geology of the Palm Desert region, Riverside Co., Calif.: unpublished senior report, San Diego State University, 24 p.

Hunt, C. W., Collins, L. G., and Skobelin, E. A., *Expanding Geospheres - Energy and Mass Transfers From Earth's Interior*: Alberta, Polar Publishing, 425 p. Order from: http://www.polarpublishing.com

Hunt, J. A., and Kerrick, D. M., 1977, The stability of sphene; experimental redetermination and geologic implications: Geochimica et Cosmochimica Acta, v. 41, p. 279-288.

Moody, J. B., Meyer, D., and Jenkins, J. E., 1983, Experimental characterization of the greenschist/amphibolite boundary in mafic systems: American Journal of Science, v. 283, p. 48-92.

Sawka, W. N., Chappell, B. W., and Norrish, K., 1984, Light-rare-earth-element zoning in sphene and allanite during granitoid fractionation: Geology, v. 12, p. 131-134.

Webb, R. W., 1939, Large sphene crystals from San Jacinto Mountains, California: American Mineralogist, v. 24, p. 344-347.

Whitney, P. R., and Olmsted, J. F., 1988, Geochemistry and origin of albite gneisses, northeastern Adirondack Mountains, New York: Contributions to Mineralogy and Petrology, v. 99, p. 476-484.